NTNU
Norwegian University of
Science and Technology

Comparison of impulse noise measurements and calculations by noise prediction methods: ISO 9613-2, NMPB-2008, Nord2000 and Harmonoise

Mary Paula Cruz Gonzalez

Problem Description

To determine the impact on communities of noise sources, such as ground and air traffic, industry, and shooting ranges, noise maps are calculated using one of a range of different methods. These methods treat the various aspects of sound propagation, such as the effect of terrain, meteorology, and reflections, in different ways. The topic of this master's thesis will be comparing such aspects between different methods by quantitative calculation for a few different cases, in particular cases that are relevant for predicting the noise from shooting ranges.

Abstract

This master's thesis presents a comparison between impulse noise measurements and calculations from four well-known propagation models; ISO 9613-2, NMPB-2008, Harmonoise and Nord2000. The calculated values are compared to two independent measurements series where the propagation path distances varied between $20\,\mathrm{m}$ and $2\,\mathrm{km}$. Meteorological conditions during the measurements were not measured in the immediate vicinity of the measurements, but collected from weather stations in the area. Measurements were carried out by Forsvarsbygg and details are not included in this report.

The comparison between measurements and calculations is done by computing the error level, i.e. the difference between measurements and calculations. Overall the results did not show any clear pattern of dependency between the error level and the different models or cases of propagation. However, the average of the results showed that, in the absence of on-site meteorological information, NMPB-2008 on average predicts the sound levels better than the other models.

This project report provides a foundation for further research and several improvements can be done in order to obtain more reliable results.

Sammendrag

Denne masteroppgaven presenterer en sammenligning mellom målinger av impulsstøy og beregninger fra fire propagaringsmodeller; ISO 9613-2, NMPB-2008, Harmonoise og Nord2000. De beregnede verdiene er sammenlignet med to uavhengige måleserier hvor propageringsavtand varierte mellom 20 m og 2 km. De meteorologiske forholdene ble ikke målt i umiddelbar nærheten av målingene, men samlet fra værstasjoner i området. Målingene ble utført av Forsvarsbygg og detaljer er ikke inkludert i denne rapporten.

Sammenligningen mellom målingene og beregninger utføres ved å beregne feilnivået, dvs. diffansen mellom målinger og beregninger. Generelt viste ikke resultatene noe klar sammenheng mellom feilnivået og de forskjellige modellene eller tilfellene. Imidlertid viste gjennomsnittet av resultatene at uten presis meteorologisk informasjon på stedet, anslår NMPB-2008 i gjennomsnitt lydnivåene bedre enn de andre modellene.

Denne rapporten gir grunnlag for videre forskning, og flere forbedringer kan gjøres for å oppnå mer pålitelige resultater.

Acknowledgements

Contents

Chapter 1

Introduction

Impulsive noise [1] as a source is complex, and often more difficult to evaluate than continuous noise e.g. industry or traffic noise; which has a longer duration in time and remains stable over a longer period of time. However, impulsive noise is characterized by high pressures and short duration, such as explosions or firing of weapons. These noise sources are very loud and can propagate long distances, being one of the major challenges when studying the sound propagation of impulse noises.

Through the last years, the study of sound from shooting ranges has been of considerable interest in environmental acoustics. In Norway, there are strict regulations and the most relevant regulation for noise limits is T-1442/2012 [2]. It defines a red zone where the establishment of noise-sensitive buildings shall be avoided, and a yellow zone where new noise-sensitive buildings may be constructed if mitigation measures provide satisfactory noise conditions. Thus, it is important to be able to predict and calculate how such noises propagate in the atmosphere. The study of impulse noises is, therefore, a good place to start in this investigation.

However, the propagation of impulse noises in the atmosphere are also affected by several time-varying factors. The theory of sound propagation in the atmosphere is well explained in several books and articles [3, 4]. According to mentioned literature, the main factors that affect sound propagation are geometrical spreading, ground effects, diffraction and meteorology. Thus, accurate calculations of sound levels in the atmosphere, and over long distances are necessary to get realistic results that can be compared with the above-mentioned noise regulations.

There are various models used for mapping shooting noise around the world

and several countries have their own standardized calculation methods; such as Nordtest model [5] used in the Nordic countries or sonARMS [6] in Switzerland. However, there are many calculation methods that can be applied to different source types and can, therefore, be used when studying impulsive noises. The propagation methods are differentiated from each other by which corrections they take into account and how these corrections are calculated. The latest methods are expected to give more accurate results than old methods, especially in complex situations. The models studied in this master's thesis are ISO 9613-2, NMPB-2008, Harmonoise and Nord2000.

ISO 9613-2 [7] is an international standard prepared by an international group of experts in 1996. Even though this method is relatively old, it is still in use in several countries. ISO 9613-2 is an empirical method based on experiments rather than physics. This is a disadvantage since the model may not fit well for cases that are not similar enough to the experiments. On the other hand, Harmonoise [8, 9] and Nord2000 [10, 11, 12] are more advanced calculation models based on physical theory. They take into account parameters and conditions that other methods cannot handle, such as complex terrain profiles and weather conditions. The Nord2000 model is widely used in the Nordic countries and Harmonoise is more recent and is the result of a cooperation between a number of European countries. NMPB-2008 [13, 14] is a French standard similar to ISO 9613-2, relatively simple and straightforward engineering model. This model was originally developed for traffic noise, but the last years has been applied to other source types.

Although these models have been extensively validated for a variety of cases, few studies have been done beyond their main application field. Several reports and articles comparing propagation models with measurements and/or reference data have been published earlier. Some relevant articles for this master's thesis are the following:

- [15] compares predicted sound levels by ISO 9613-2, NMPB-2008 and Harmonoise and experimental data which cover typical road configurations.

- [16] compares calculations from Harmonoise and Nord2000 with reference data from the literature and from measurements controlled by a computer program.

- [17] where road traffic is studied by comparing calculations from commercial software programs and field measurements. The main purpose was to determine how well the programs predict the sound levels.

This report aims to investigate the uncertainty and variation in predicted sound levels computed based on the outdoor sound propagation models ISO

9613-2, NMPB-2008, Harmonoise and Nord2000. The purpose is to determine if the models can give accurate enough results when studying the propagation of impulse noises on short and long distances in the atmosphere.

1.1 Structure of the Report

This report is constructed in the following order: Chapter 2 gives a brief introduction to the principal effects that affect the sound propagation in the atmosphere. In addition, an overview of the different propagation models is presented. Chapter 3 describes the method used to do the comparisons between measured and calculated sound levels at different receiver points. As well as a short description of the measurement setup. Chapter 4 presents the results from measurements and comparisons. In Chapter 5, a discussion of the results from measurements and calculations is given. Chapter 6 presents final conclusions and suggestions for future work.

Chapter 2

Theoretical background

In this chapter fundamentals of outdoor sound propagation are described, giving an overview of the most significant parameters that affect the propagation in the atmosphere. In addition, a description of the four sound propagation models studied in this thesis is presented.

2.1 Sound propagation in the atmosphere

The propagation of sound in the atmosphere is complex. The main factors that affect sound propagation in the atmosphere are geometrical spreading, ground effects, diffraction, and meteorological effects. These factors are briefly discussed in the following sections, and more details can be found in the literature [3, 18, 19].

2.1.1 Geometrical spreading

Geometrical spreading refers to how sound level decreases as a sound wave propagates away from a source. The amount of attenuation depends on the type of the sound source and the distance from the source. Further in this master's thesis, it is assumed that sources are point sources that generates spherical waves. The amplitude of a spherical wave decreases as $1/r$ with increasing distance from the source, where r is the distance from the source. This implies that sound level is reduced by $6\,\mathrm{dB}$ per doubling of distance from the source [19]. In a homogeneous atmosphere, the geometrical atten-

uation, ΔL_d, corresponding to spherical spreading is given by the following equation:

$$\Delta L_d = 10 \log 4\pi r^2 \qquad (2.1)$$

2.1.2   Meteorological effects

Outdoor sound propagation is strongly affected by atmospheric conditions especially at longer distances. The three most significant meteorological effects on sound propagation are atmospheric absorption, refraction, and scattering by turbulence. These factors will be briefly discussed in following sections.

Atmospheric absorption

In a real atmosphere, the decrease in the amplitude of a spherical wave is larger than in a homogeneous atmosphere due to the effect of atmospheric absorption. The atmospheric absorption is caused by two main effects: i) heat conduction and shear viscosity, and ii) molecular relaxation [3]. These loss components vary with the temperature, atmospheric pressure, and humidity. The attenuation, in decibels, due to atmospheric absorption can be expressed as:

$$A_{air} = \alpha r \qquad (2.2)$$

where α is the absorption coefficient and r is the distance from the source in meters. The absorption coefficient depends mainly on the frequency, temperature, and humidity of the atmosphere. Atmospheric absorption increases linearly with distance and becomes more important on long-range outdoor sound propagation. For small distances and low frequencies, the absorption can be neglected [3].

Atmospheric refraction due to temperature and wind

Refraction is a change of the propagation direction of a sound wave caused primarily by vertical gradients of the temperature and wind speed. The wind and temperature gradients have a large effect on the propagation of sound through the atmosphere, especially when the propagation distances are greater than a few hundred meters. For small distances, it can be assumed a non-refracting atmosphere.
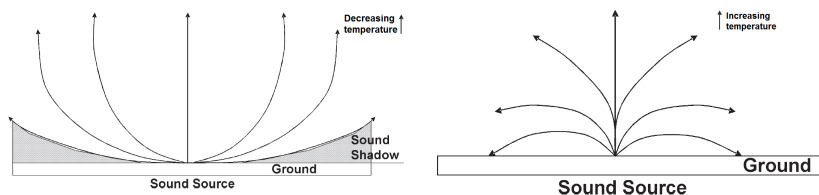
(a) Downward refraction caused by a positive temperature gradient

(b) Upward refraction caused by a negative temperature gradient

Figure 2.1: Atmospheric refraction due to temperature variations [16]

The sound speed depends mainly on the temperature; higher temperatures give a higher speed of sound. In the atmosphere, the temperature is not uniform causing spatial variations in the sound speed. In other words, the direction of the propagation changes when sound propagates at different velocities; bending the waves upwards or downwards. This effect is known as refraction. Downward refraction, as shown in Figure 2.1b, occurs if the sound speed or temperature increases with altitude (positive temperature gradient). The result is higher noise levels near the ground compared to a non-refraction atmosphere. This effect is typical at night or in winter and is the reason why sound sometimes can be heard over considerable distances at night. The opposite occurs when the temperature decreases with altitude (negative temperature gradient), the sound waves will bend upward, reducing the sound level near the ground, and forming a shadow zone as shown in Figure 2.1a [20].

The influence of wind also affects sound propagation through the atmosphere, and the effects can be similar to temperature effects. Wind gradients refer to the change in wind speed over relatively short distances. This effect commonly occurs due to the fact that wind closer to the ground moves slower because of the friction and obstacles from the ground. With increasing height, the effect of friction decreases, so the wind speed increases. Therefore, when sound propagates with the wind, sound waves closer to the ground travels slower and the rays are curved downward as shown in Figure 2.2b. If sound propagates against the wind, the speed of sound will be reduced by the wind speed, resulting in a lower speed in the upper region. Sound waves will then be refracted upwards, creating a shadow zone near the ground as shown in Figure 2.2a.
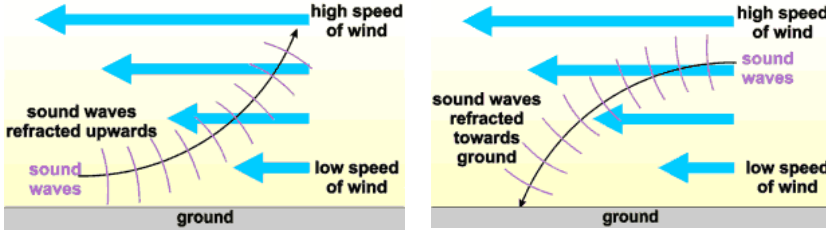
(a) Upward refraction due to upwind propagation

(b) Downward refraction due to downwind propagation

Figure 2.2: Atmospheric refraction due to wind speed variations [16]

Scattering due to turbulence

Turbulence refers to irregular air motions characterized by winds that vary in speed and direction. When sound propagates through the atmosphere, these random fluctuations scatter sound into sound shadow zones, causing a large increase in the levels in a shadow region as shown in Figure 2.3. Additionally, turbulence causes fluctuations of the phase and the amplitude of the sound waves. Turbulent phase fluctuations are very important for the interference minima in the spectrum. An interference minimum occurs at a frequency where direct and reflected waves have a phase difference of 180° and (partially) cancel each other. The phase fluctuations of the direct and reflected waves thus cause random fluctuations of the frequency of the interference minima. The effect of scattering due to turbulence is very complex and more details can be found in [3, 21].
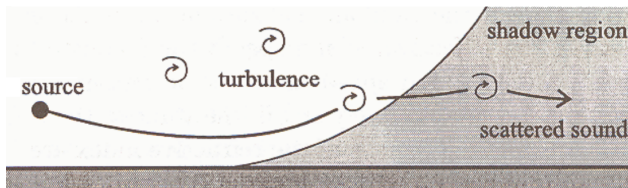

Figure 2.3: Scattering of sound into shadow zone [3]

2.1.3   Ground effects

Sound waves can propagate directly to the receiver or be reflected and/or absorbed by the ground. The sound pressure level at the receiver is then the contribution of the direct and reflected sound waves. The source-receiver

geometry is illustrated in Figure 2.4.

The amount of energy absorbed and/or reflected depends on the frequency of the sound, the propagation distance, the surface characteristics, and the angle of incidence, θ. Usually, the ground surface is characterized by its absorption coefficient or the acoustic impedance of the surface. Hard and smooth surfaces with practically infinite impedance, such as concrete or water, will reflect the wave entirely, meaning no absorption. Soft surfaces like grassy ground have a higher absorption, attenuating the sound level significantly.
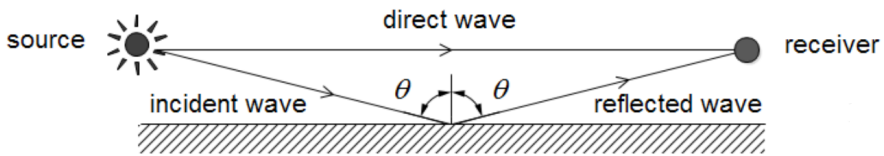

Figure 2.4: Reflection of a sound wave on a flat reacting ground surface [21]

The reflected waves leave the surface at the angle of incidence of the wave, as shown in Figure 2.4. The amplitude and phase of the wave are modified by the impedance of the surface. These reflections can interfere with incident waves causing constructive or destructive interference. Destructive interference occurs if the phase of the reflected and direct sound has opposite signs, canceling each other and reducing the sound level in the receiver position. This occurs especially when the source and the receiver are close to the ground. Constructive interference refers to reflections in phase with direct sound, increasing the sound level at the receiver [3].

2.1.4 Diffraction

Diffraction is the phenomenon that occurs when sound waves bend as they propagate around obstacles or through openings, as shown in Figure 2.5. The diffraction effect depends on the wavelength of the sound wave and the size of the object. Lower frequencies sounds have larger wavelengths that are longer than most objects size, resulting in larger diffraction effect. When the size of the gap or obstacle is comparable in size to the wavelength of the wave, typically high frequencies, no diffraction occurs, creating a shadow zone behind the barrier. Therefore, a barrier is generally more effective in attenuating the higher frequencies as compared with the lower frequencies.
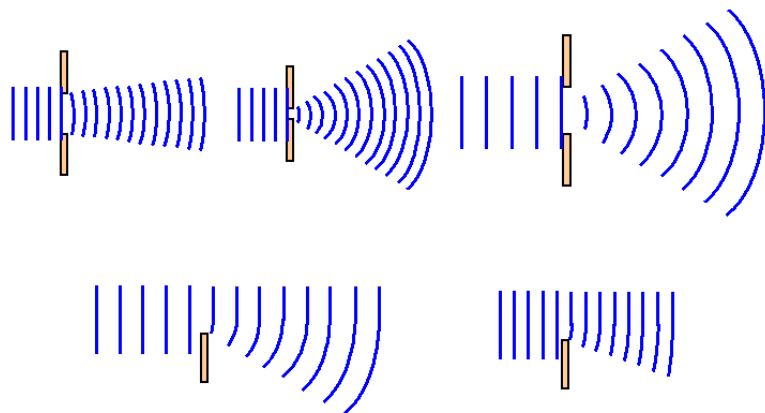
Figure 2.5:   Examples of wave diffraction showing the connection between wavelength and size of the barrier or gap [22]

2.2   Sound prediction models

Several computational models have been developed to predict the sound propagation in the atmosphere. Noise prediction models are typically built around a common framework. The sound pressure level $L_{p,k}$, in decibels, at a receiver point is given by Equation. 2.3.

$$L_{p,k} = L_{W,k} + \sum_i \Delta L_{i,k} \tag{2.3}$$

where the subscript k refers to the frequencies, $L_{W,k}$ is the sound power level within the considered frequency band, and $\sum_i \Delta L_{i,k}$ is the sum of corrections and attenuation due to propagation. Some of the corrections used in most of the models are the attenuations as a result of the geometrical spreading, air absorption, meteorological effects, terrain or ground effects, barriers and reflections. What differentiates these models is which corrections they take into account and how each of these corrections is calculated.

The following sections present an overview of four widely used propagation models. The most relevant features for this thesis are described and compared to each other. More details of each model can be found in their own model description. The four models are ISO 9613-2, NMPB-2008, Nord2000 and Harmonoise.

2.2.1 ISO 9613-2

ISO 9613-2 [7] is an international standard that specifies a method for calculating the attenuation of sound propagating outdoors. ISO 9613-2 is an empirical method which means that it is based on previous observations and experiments rather than physics. The standard ISO 9613-2 is applicable to a wide variety of ground-based noise sources and environments. Although ISO 9613-21 was published in 1996, this standard is still used in several countries to predict sound pressure levels at distance positions up to the order of 1 km. Additionally, ISO 9613-2 and the Nordtest method (NT ACOU 099 [5]) used in the Nordic countries for shooting noise are very similar and will predict very similar sound levels in most cases [23].

The calculations are computed for octave bands from 63 Hz to 8 kHz. The method predicts both the equivalent continuous A-weighted sound pressure level and a long term average A-weighted sound pressure level. The equivalent continuous sound pressure level is the average sound pressure level during a period of time under favorable meteorological conditions (downwind propagation). While the long term average sound pressure level is calculated over a significantly longer period encompassing a wide variety of meteorological conditions.

The precision of the ISO 9613-2 is stated to be ± 3 dB for distances up to 1 km. Accuracy for distances larger than 1 km is not discussed in the standard, such distances are important when studying shooting noises. Furthermore, ISO 9613-2 takes into account source type and directivity, geometrical spreading, atmospheric absorption, ground effect, reflection from surfaces and screening by obstacles.

Ground effects

The total ground attenuation in ISO 9613-2 is given by the sum of the ground attenuation of three distinct regions: the source region, a middle region and the receiver region, each of which are characterized by a ground factor G. For hard ground $G = 0$; for porous or soft ground $G = 1$; and for mixed ground $0 < G < 1$. This method is applicable only to ground which is approximately flat, either horizontally or with a constant slope.

For ground surfaces of irregular shape, the ground attenuation is calculated from an equation given in the ISO 9613-2 standard [7]. This equation is based on the mean height, h_m, of the propagation path above the ground (see Figure 2.6), and the distance between the source and the receiver, in meters.
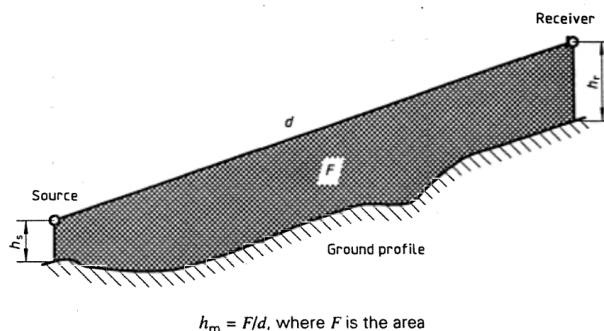
Figure 2.6: Method for evaluating the mean height [7]

Meteorological conditions

One of the limitations of the ISO 9613-2 standard is that it assumes moderate downwind conditions; wind speed between approximately $1\,\mathrm{m/s}$ and $5\,\mathrm{m/s}$, and wind direction within an angle of $\pm 45°$. ISO 9613-2 suggests an optional simple correction to calculate the long-term average A-weighted sound pressure level, L_{AT}, which encompasses both favorable and unfavorable conditions. L_{AT} is calculated by reducing the predicted short-term downwind levels with a meteorological correction, C_{met}, less than 5 dB, given by local meteorological statistics for wind speed and direction, and temperature gradients.

Reflections

In this standard, these reflections refer to reflections from obstacles, e.g outdoor ceilings and more or less vertical surfaces, which can increase the sound pressure levels at the receiver. Reflections from the ground are included into the calculation of ground effects.

Reflections are taken into account only if all the following requirements are fulfilled: i) a specular reflection can be constructed, ii) the magnitude of the sound reflection coefficient for the surface of the obstacle is greater than 0.2 and, iii) the surface is large enough for the nominal mid-band wavelength, λ, in meters.

The reflections from an obstacle are calculated for all octave bands according to the mirror image method and by using a surface-dependent reflection coefficient. The real source and source image are handled separately, as two sources at two different positions. The attenuation terms and sound power level are calculated according to the propagation path of the reflected sound [7].

Diffraction

According to the ISO 9613-2 standard, objects which obstruct the propagation of sound shall be represented by a barrier with vertical edges if the object has the following characteristics: i) the surface density of the object is greater than $10 \, \text{kg/m}^2$, ii) the object has a solid surface without large cracks or gaps and, iii) the horizontal dimension of the object perpendicular to the source-receiver line is larger than the acoustic wavelength, λ.

The attenuation by a barrier is then given by the insertion loss, which means the difference, in decibels, between the sound pressure levels at a receiver with and without the barrier. ISO 9616-2 allows to estimate the attenuation both around the vertical edges and over the top edge of the vertical sound barrier. If one of the attenuations is insignificantly, ISO 9613-2 will assume that only one significant sound propagation path exists.

Screening can be calculated for single or multiple screens or single screens with finite thickness. When calculating the effect of more than two barriers, only the two most effective barriers are taken into account, ignoring the effect of the others. ISO 9613-2 suggests limiting the maximum attenuation calculated to 20 dB in case of single screens, and 25 dB for multiple screens.

2.2.2 NMPB-2008

NMPB-2008 [13] is a French standard similar to ISO 9613-2, but some of its features are more developed. This method was originally intended for the prediction of the propagation of road traffic noise. However, the method can easily be adapted subsequently to railway and industrial noise.

This model is a simplified engineering method because it employs several empirical approaches. One advantage of this method over the ISO 9613-2 standard, is that NMPB-2008 takes the meteorology into account based on a huge database of meteorological measurements obtained from different meteorological stations over a period of around 20 years.

The calculations are computed for one-third octave bands from 100 Hz to 5 Hz. Unlike the ISO 9613-2 method, NMPB considers both favorable or downward-refraction propagation (positive vertical gradient); and homogeneous atmospheric conditions (zero vertical gradient) over the entire propagation area. The two types of meteorological conditions are weighted by the probability of occurrence of favourable conditions.

NMPB-2008 computes a long term sound level based on two computations, one for homogeneous conditions and one for favourable conditions.

Ground effects and diffraction

In NMPB-2008, the description of ground and attenuation due to diffraction are computed as in the ISO 9613-2 standard. The description of the ground is based on the concept of mean ground plane as shown in Figure 2.6. Diffraction is computed by the image source method where two mean ground planes are considered, i.e. one on each side of the diffraction point, as illustrated in Figure 2.7). The ground is described as in the ISO 9613-2 model; by a frequency independent parameter G between 0 and 1. In contrast to the ISO 9613-2 model, the ground absorption in NMPB-2008 is computed by the average of G along the mean ground plane between source and receiver.
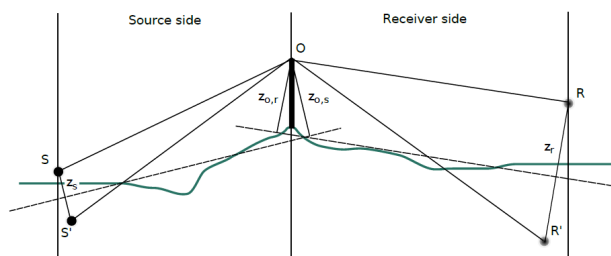

Figure 2.7: Geometry of calculating the attenuation from diffraction [13]

2.2.3   Nord2000

The Nord2000 method was developed by DELTA (Denmark, project manager), SINTEF (Norway), and SP (Sweden). Nord2000 is an advanced calculation method for prediction of noise propagating outdoors. This model is not based on experiments as ISO 9613-2 and NMPB-2008, but in physical theory. The model predicts the sound pressure level at the receiver in one-third octave bands from 25 Hz to 10 kHz based on Equation 2.3.

The propagation model is applicable to a variety of noise sources, and covers most mechanisms of attenuation. For noise sources close to the ground, the method is intended to be used for propagation distances up to approximately 1 km [12]. Nord2000 is a very comprehensive model, having several advantages over other methods. It takes into account parameters and conditions that other methods cannot handle. Some of these are described in the following sections:
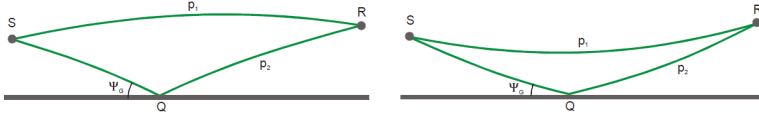
Figure 2.8: Sound rays for flat terrain in case of downward refraction (left), and upward refraction (right) [12]

Meteorological conditions and refraction

One of the main advantages of the model is that it can be applied for a variety of weather conditions. In a homogeneous atmosphere (without significant refraction and constant sound speed), the model assumes that sound rays follow straight lines. In an atmosphere with moderate refraction, the model assumes that the sound speed varies linearly with the height above the ground and the straight lines are replaced by curved sound rays simulating the actual phenomenon of refraction, as shown in Figure 2.8. The curvature depends on the sound speed profile and is determined by a semi-analytical approach [11].

In reality, the sound speed profile in the atmosphere is more complex, and does not necessarily vary linearly. When the sound speed profile is non-linear, it can be represented by sound speed profiles with a logarithmic and a linear part called log-lin profiles as shown in Equation. 2.4.

$$c(z) = A \ln \left(\frac{z}{z_0} + 1 \right) + Bz + C \tag{2.4}$$

where z_0 is the roughness length, in meters, C is the sound speed at the ground and A and B are weather coefficients determined from weather data available. The logarithmic part is determined by the wind speed and wind direction while the linear part is determined by the temperature and is assumed to increase linearly with the altitude. C is determined by the air temperature (see [10] for further details).

In case of strong downward refraction the model has been extended to include the effect of additional rays from multiple reflections. In case of strong upward refraction, where no ray will reach the receiver in a shadow zone, the model has been extended to include effects of shadow zones.

Other meteorological parameters defined in Nord2000 are the turbulence strength (corresponding to wind and temperature), humidity, standard deviation of the wind speed and fluctuations in the temperature gradient.
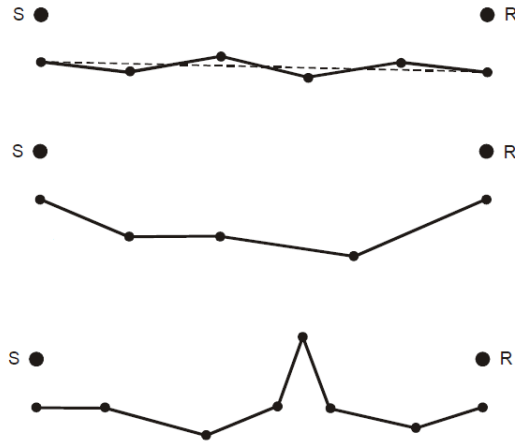
Figure 2.9: Examples of segmented terrain: moderately non-flat terrain, valley-shaped terrain and terrain with a screen [24]

Ground effects

Nord2000 is applicable for any terrain shapes with or without screens. The terrain is represented by a sequence of straight line segments, as shown in Figure 2.9, where each segment is defined by its roughness, σ_r, and flow resistivity, σ, or impedance.

The roughness parameter is a quantification of the unevenness of the terrain segment. A classification has been made for roughness types which includes four roughness classes. The classification is described in the Nord2000 description [10]. The ground impedance is described by the Delany and Bazley impedance model [25], where the impedance of a ground surface is calculated based on the frequency and flow resistance. Unlike other methods that characterize the ground properties either as soft or hard, Nord2000 defines eight different impedance categories which include a number of ground types representing typical surfaces [25, 10].

In the Nord2000 propagation method, the Fresnel-zones are used when predicting the effect of ground properties on the reflected sound, see Figure 2.10. When sound is reflected by a plane surface with varying surface types, the efficiency of the reflection is computed by the ratio between the area of the surface within the Fresnel-zone and the area of the entire Fresnel-zone. The size of the Fresnel-zones is frequency dependent [26, 12].

The ground effect is calculated for each type of ground to be found inside the Fresnel-zone and the resulting ground effect is calculated as a weighted
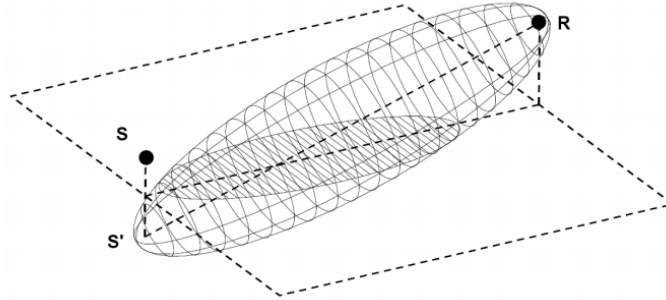
Figure 2.10: Definition of Fresnel ellipsoid and Fresnel-zone [12]

average taking into account the fraction of the Fresnel-zone covered by each type of ground surface [27].

2.2.4 Harmonoise

Harmonoise is another engineering model for predicting environmental noise levels very similar to the Nord2000 model.

Harmonoise predicts the sound pressure level in one-third octave bands from 25 Hz to 10 kHz. This method computes a long time average value. In addition, it handles different meteorological conditions, and it is also applicable to multiple source types as road, railway.

Ground profile and effects

The ground geometry and effects are computed by using the same methods as in the Nord2000 method. The model is applicable for any terrain shapes approximated by a segmented terrain shape with or without screens as shown in Figure 2.9. In contrast to the Nord2000 model, Harmonoise does not define a roughness parameter for each segment. In Harmonoise, the ground surface properties are defined by the acoustic impedance of the ground. The ground impedance is computed based on the the Delany and Bazley impedance model [25], which is characterized by the flow resistance of each ground segment. The effect of the terrain properties on the reflected sound is also computed by using the Fresnel-zone model as in the Nord2000 model.
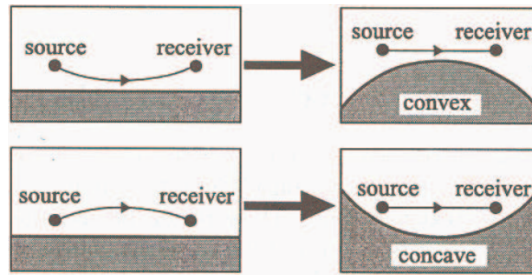
Figure 2.11: Curved ground analogy used by the Harmonoise model [3]

Meteorological conditions and refraction

As in the Nord2000 model, Harmonoise allows different weather conditions
by approximating the vertical sound speed profile by a lin-log relationship.
However, the atmospheric refraction is handled in different ways by these
two methods. Harmonoise uses straight rays and curves the ground in the
opposite way as rays are curved. The radius of curvature is calculated from
the maximum height of the curve, which is a simpler method than the one used
in Nord2000. The curved ground analogy used by Harmonoise is illustrated
in Figure 2.11.

The effect of scattering by atmospheric turbulence is taken into account by
adding a scattering term to the the excess attenuation. This term increases
with increasing the distance.

Chapter 3

Methodology

This chapter describes the methodology used in this project to process the data and evaluate the different models by comparing field measurements and values calculated by the sound propagation models. The main purpose is to determine the precision of the models for the cases studied.

3.1 Field measurements

Two measurement series were carried out by Forsvarsbygg in order to evaluate the sound propagation of impulsive noise. Both measurement series were performed in Rena/Åmot, Hedmark, on the outskirts of the city. These were carried out in two different periods of the year so that there was a change in the weather conditions. Noise levels were measured approximately every two minutes in all the receivers.

The source used in the experiments was a gas cannon of the model DBS E Auto Cannon, see Figure 3.1. The cannon generated impulsive high sound levels, firing approximately every 2 minutes. The mouth of the cannon was placed at a height of $0.5\,\mathrm{m}$ above the ground and the microphones at $2\,\mathrm{m}$ high.

The first measurement series was done in October 2015. Measurements were done at five different positions. In four of them the measurements were taken over 2 days and 19 hours. In the last receiver, measurements were taken over less than a day. The source and microphones were placed more or less on a straight line as shown in Figure 3.2. Distances between the source and the

Figure 3.1: Gas cannon of model DBS E Auto Cannon used as the source in field measurements [28]

microphones vary from 25 m to approximately 2 km.

The second measurement series was done in July 2016 over 3 days and 22 hours. The microphones were placed around the source at a distance of approximately 1 km from the cannon, see Figure 3.3.

In addition, the meteorological data at the same time of the measurements was collected from five different weather stations around the measurement area. The weather station nearest to the measurement area was Tørråsen, located around 2 km away, while the other stations are between 1 km–15 km from the source, as shown in Figure 3.4.

3.2   Data

The measurement data sent by Forsvarsbygg consists of three Matlab files:

1. KanonData.mat which contains source calibration measurements in one-third octave frequency band for five different angles; 20 measurements at angles 0°, 45°, 90°, 135° and 180°.

2. WeatherStruc.mat which contains measurement data from meteorological stations nearby the measurement area. WeatherStruct is a 2D-array with the two measurement series along the first dimension, and different weather stations along the second dimension. In each weather station, wind speed, wind direction, humidity, air temperature, wind gust, rain and air pressure were measured every ten minutes.

3. DataStruct.mat contains measurements taken every 2 minutes from the various microphones around the source. DataStruct is also a 2D-array
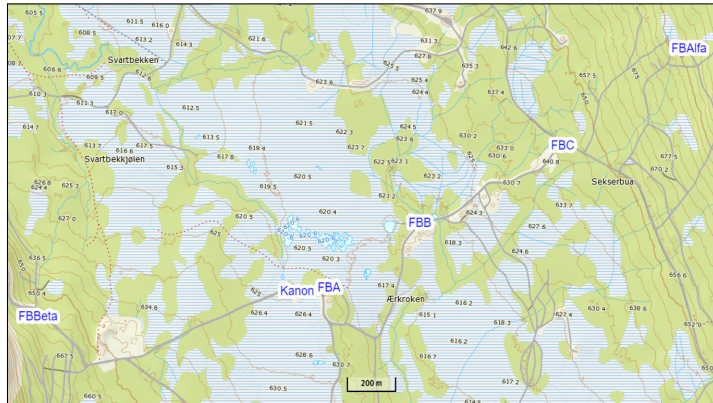
Figure 3.2: Measurement set-up in series 1. Distances between sound source (Kanon) and receivers are as follows: Kanon-FBA≈25 m, Kanon-FBB≈450 m, Kanon-FBC≈1100 m, Kanon-FBAlfa≈1700 m, Kanon-FBBeta≈1100 m
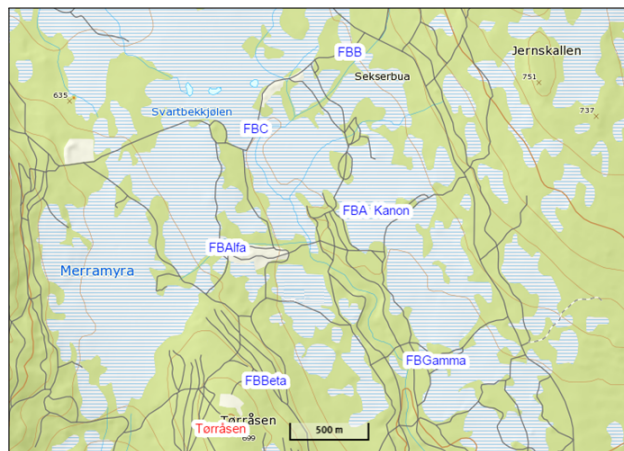

Figure 3.3: Measurement set-up in series 2. Distance between sound source (Kanon) and receiver FBA is 30 m. Distance between Kanon and the other receivers is approximately 1 km
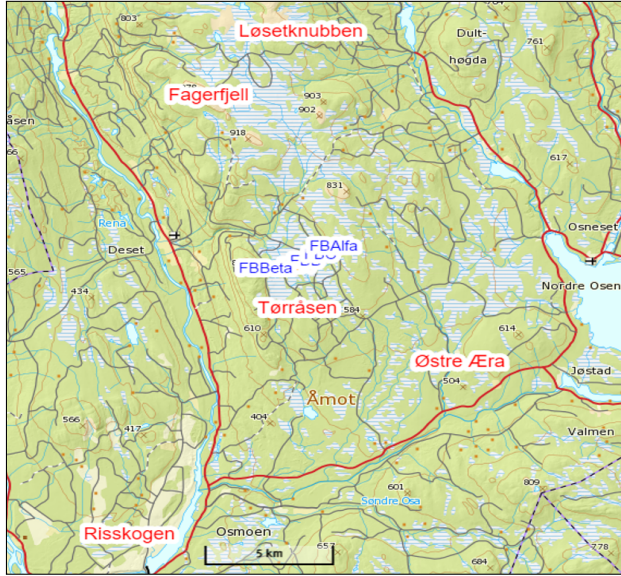
Figure 3.4: The figure shows the weather stations, in red colour, where the meteorological data was collected

with the two measurement series along the first dimension, and different microphones/receivers along the second dimension. The data measured in each receiver consists of fast and impulsive A-weighted sound levels, and fast frequency weighted in one-third octave bands from 0.4 Hz to 20 kHz. Additionally, the position and angle of each receiver and source are given. The position is given in the Universal Transverse Mercator (UTM) format which is a 2-dimensional Cartesian coordinate system [29]. A position on the Earth is given by the UTM zone number and two numbers, the easting and northing coordinates. In this case, the UTM zone number is 32 which represents the southeast Norway, and the coordinates are different for each source and receiver. The angle of the sources and receivers refers to the angle relative to the true north direction, and is given in degrees. The exact date and time of each measurement are given as serial date numbers (Matlab's datenum format), and are also included in this structure array.

During the measurements, the clocks on the receivers were not fully synchronized. By assuming that the clock in receiver nearest to the cannon (receiver 1-FBA) was correct, and by comparing with the first measurements in the other receivers, it appeared to be only few seconds difference in receivers FBB and FBC in both measurement series. While in the other receivers (FBAlfa,

FBBeta and FBGamma) it was recorded 70 seconds error in the first series and almost one day (86396 seconds) in the second measurement series. This correction was taken into account by changing the date/time of the measurements by -3, -5, -71 and -70 seconds for receivers FBB, FBC, FBAlfa and FBBeta, respectively, in series 1. In series 2, the corrections were -3, -2, 86396, 86396, 86396 seconds for receivers FBB, FBC, FBAlfa, FBBeta and FBGamma, respectively.

In order to get the most accurate results when comparing calculations with measurements, the data was split into chunks of several measurements. This was done by choosing the measurements taken in the same time period as the weather condition measurements.

The processing of the data was done in Matlab, and boxplots were used to present the data in order to get a better understanding of the distribution and variation.

3.3 Terrain profile

Since the data included only the UTM-coordinates of the receivers and sources, the terrain profile between the sources and each receiver was found from Kartverket's map data using SINTEF's TAdll library. This gives an approximation of the elevation profile between two UTM-coordinates. In addition, Norgeskart [30] was used to determine the ground characteristics of the propagation path. An example of a terrain profile obtained from Norgeskart is shown in Figure 3.5. Based on this information, the terrain profile between the source and each receiver was approximated by a number of straight line segments depending on the form and ground type as shown in Figures 3.6 and 3.7.

3.4 Calculation of sound levels

The total sound pressure level in the receiver points was computed based on Equation 2.3, and two implementations: Nord2000 and CNOSSOS-EU.

The Nord2000 results were obtained based on a Matlab program called ComproABC21.m, i.e. the 18th version of the code. The program calculates the sound pressure level in one-third octave bands relative to the free field sound pressure level, ΔL. In other words, the sound pressure level, ΔL, is the result of extra power due to ground/reflection effects, weather conditions and air absorption. The input data to the Nord2000 program are several paramet-
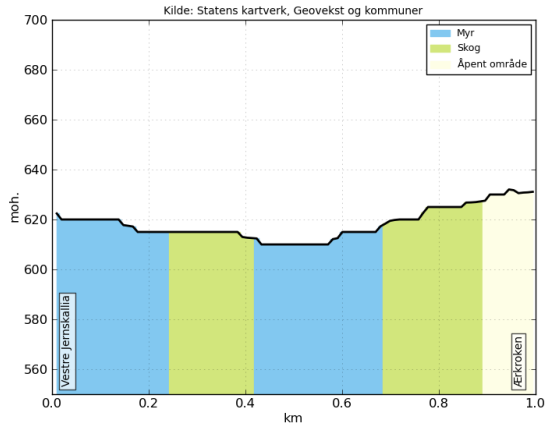
Figure 3.5: Example of a terrain profile from Norgeskart showing information about the ground surface. Where blue color refers to marsh, green represents forest areas, and egg white color refers to an open area
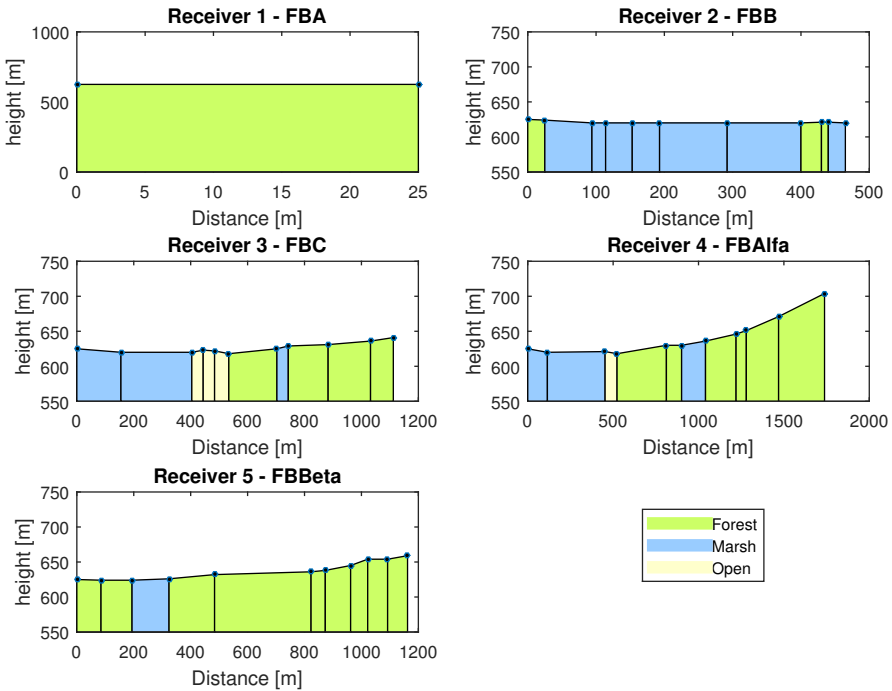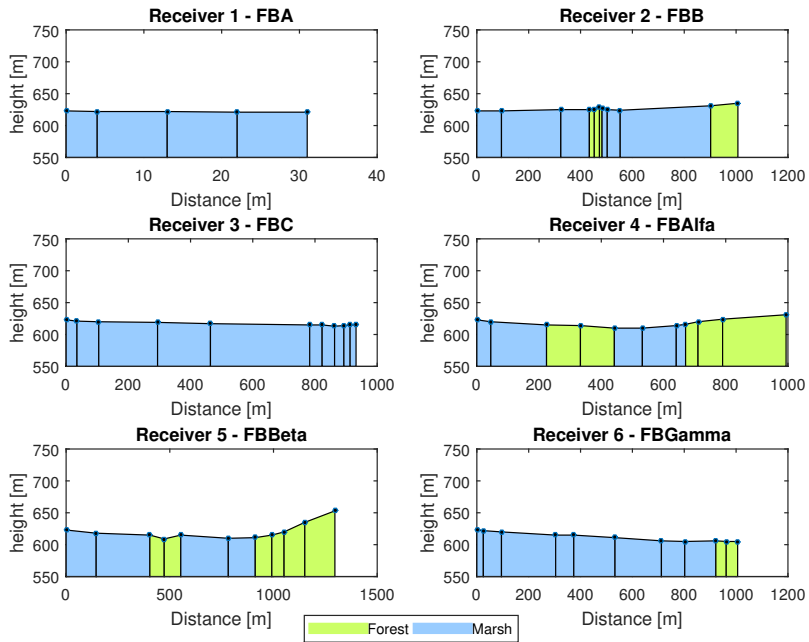

Figure 3.6: Segmented terrain profiles for series 1

Figure 3.7: Segmented terrain profiles for series 2

ers that together give a complete description of the terrain and atmospheric conditions.

CNOSSOS-EU is an implementation that allows to calculate the sound pressure level for octave frequency bands based on three different propagation models: ISO 9613-2, NMPB-2008 and Harmonoise. All three propagation models can be run based on a single set of input data. The input to the propagation modules is a XML-file which contains a geometrical description of the propagation path in 2D coordinates, associated material properties, sound power level of the source, and a few meteorological parameters. Meteorological data in CNOSSOS is taken into account by calculating sound levels in favourable and homogeneous conditions, if available for the selected method. More details about the implementation of CNOSSOS-EU can be found in [31].

The following sections describe how these implementations are used to calculate the total sound pressure level at different distances from the source.

3.4.1   Nord2000

As mentioned before, the Nord2000 implementation calculates the sound pressure level relative to the free field, which refers to attenuation due to reflections, ground and atmospheric effects. In order to calculate the total sound pressure level in a receiver, the following equation was used:

$$L_{p,k} = L_{W,k} - \Delta L_d + \Delta L_k \tag{3.1}$$

where $L_{W,k}$ is the sound power level of the source including directivity correction, ΔL_d refers to the geometrical spreading of a point source given by Equation 2.1, and ΔL_k is the sound pressure level calculated by the Nord2000 implementation. The subscript k refers to the frequencies in one-third octave bands.

In the following sections a description of how ΔL and L_W were computed is presented.

Sound pressure level relative to free field, ΔL

In order to be able to run the program, all input parameters had to be assigned. Some of the parameters could be set directly, but others were calculated or estimated. The input parameters to the program can be divided in variables defining the terrain, the weather conditions, and optionally variables defining a scattering zone.

The parameters defining the terrain were obtained based on the terrain profiles computed in Section 3.3. Each terrain segment was defined by its flow resistivity and ground roughness. The ground flow resistivity was defined based on a classification of ground impedance types given in the Nord2000 model [10, Chapter 5]. Marsh were characterized by impedance class "B" and flow resistivity $31.5 \, \text{kNsm}^{-4}$, open areas by impedance class "C" and flow resistivity $80 \, \text{kNsm}^{-4}$ and forest by impedance class "D" and flow resistivity $200 \, \text{kNsm}^{-4}$. Each segment was assumed to be flat and ground roughness parameter was then set to $0 \, \text{m}$.

When defining the parameters that describe the weather conditions, two cases were computed. One case assuming homogeneous weather conditions. In the other case, assumptions and calculations were done based on meteorological measurements from the weather stations nearby the measurement area.

In the case of homogeneous conditions, temperature gradients, wind speed, turbulence parameters and relative humidity were set to 0.

In the other case, corrections and assumptions were done in order to estimate

necessary parameters. The air temperature and humidity in the measurement area were assumed to be the same as in Tørråsen, the nearest weather station. The temperature gradient was estimated by plotting the temperature measured in all the weather stations with respect to height. This was done without considering that the distances between the weather stations and the measurement area vary between 2–10 km, and should be weighted differently. Linear least squares fitting technique was then used to get the best fitting straight line through the set of points. The slope of this line defines the temperature gradient. Wind turbulence parameter, C_v^2, was set to $0.12\,\mathrm{Ks}^{-2}$, and $0.008\,\mathrm{m}^{4/3}\mathrm{s}^{-2}$ for the turbulence corresponding to temperature. These values are suggested in [32, Appendix 4].

When determining the sound speed profile by Equation 2.4, the roughness length z_0 was set to $0.1\,\mathrm{m}$ since the receiver or source height shall not be less than 5 times the roughness length according to the Nord2000 description document [12].

The wind speed at the receivers was estimated based on the wind direction and wind speed measured in Tørråsen. This was done by representing the wind speed and wind direction measured in Tørråsen by a vector, v_{WS}, and decomposing it into a component along the direction of the receiver, $\hat{r}_R$. The wind speed at the receiver is then given by v_R (see Figure 3.8 and Equation 3.2).

The estimated wind speed at each receiver, v_R, was computed by Equation 3.2, where v_{ws} is the wind speed measured in Tørråsen, and θ_{diff} is the angle difference between the wind direction and receiver's position.

$$v_R = v_{ws} \cos\theta_{diff} \tag{3.2}$$

Sound power level and directivity correction, $L_{W,k}$

The sound power level of the source was estimated based on the sound levels measured in the receiver nearest to the source, and the calculated values obtained from the Nord2000 implementation. Equation 3.1 was used in reverse to calculate the sound power level, $L_{W,k}$. Where $L_{p,k}$ is the frequency dependent measured value at the receiver nearest to the source (receiver 1 - FBA). ΔL_d refers to the spherical spreading at the distance of receiver 1-FBA from the source, and ΔL_k is the calculated value from the Nord2000 implementation. To obtain a sound power level that applies for all the measurements, the average of all calculated values of ΔL_k and all measured values, $L_{P,k}$ were used.

In addition, the directivity of the source had to be considered since not all the
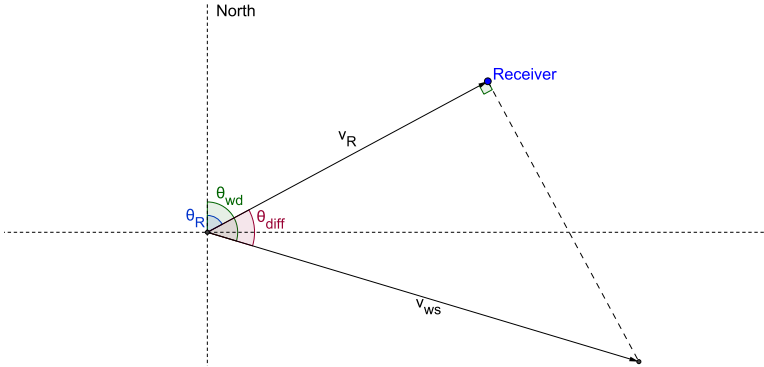
Figure 3.8: Geometry for estimating the wind speed at receivers. θ_R and θ_{wd} are the angles of the receiver and weather station relative to the north

microphones were placed in the same direction of the source. The directivity correction was estimated based on the source calibration measurements performed by Forsvarsbygg. The measurements consist of max, A-weighted values, $L_{AF,max}$ and fast frequency weighted in one-third octave bands, L_{fF}, measured 20 times at angles 0°, 45°, 90°, 135° and 180°. The average of the measurements in each angle was used to estimate the correction. The correction at other angles was computed by interpolation.

3.4.2   CNOSSOS-EU

As previously mentioned, CNOSSOS calculates the total sound pressure level in homogeneous and favorable conditions, if both are available for selected method. In addition, it also provides the individual attenuation components that correspond to the overall sound level. The program calculates the geometrical spreading, atmospheric absorption, attenuation due to reflections, diffraction and attenuation under favourable or homogeneous conditions.

In order to calculate the total sound level, the sound power level must be known. Sound power level was calculated in the same way as before, based on Equation 3.1. Where L_p is the average of all measurements in FBA-receiver and ΔL is the sum of the individual attenuation components obtained from CNOSSOS (atmospheric absorption, geometrical spreading and excess attenuation under homogeneous or favorable propagation conditions). Since the measurements are levels of one-third octave band, and calculations from CNOSSOS are octave bands levels, the measurements levels of one-third

octave band were converted to octave bands. Octave band levels were calculated by adding the one-third octave bands that together cover the same frequency range. Directivity of the source was also included, by adding a correction coefficient to the calculated sound power level. The directivity correction was computed as in the Nord2000 model.

The terrain profile was computed as in Section 3.3 by dividing the terrain into smaller segments. Each segment is described by "identifiers". The software has a predefined set of identifiers, consisting of 8 ground types and material for vertical walls. In this case, forest was described by identifier "D", marsh by "B" and open area by "C".

CNOSSOS was used to calculate the sound levels for all the three models: ISO 9613-2, NMPB-2008 and Harmonoise. A detailed explanation on how to run the program is available in the "user and programmers guide" included in the download files [31].

3.5 Comparison of calculations and measurements

The main purpose of the present work is to compare the measurements with levels calculated by different outdoor propagation models. This was done by computing the difference between measurements and calculations for each propagation model and for all the receiver locations. The error level or difference was calculated by $L_{error} = L_{A,meas} - L_{A,calc}$. In order to obtain a good overview of the results, boxplots computed in Matlab [33] were used to present most of the results. Section 3.5.1 gives a short explanation of what the different parts of the boxplots describe.

In addition to the graphical results presented by boxplots, the average error level, L_{avg}, from each model was computed by Equation 3.3. Where $|L_{N,error}|$ refers to the absolute value of the median of error level for each case, N.

$$L_{avg} = \sum_N \frac{|L_{N,error}|}{N} \qquad (3.3)$$

3.5.1 Boxplot

In a boxplot, see Figure 3.9, the front and back edges of the box indicate the first (Q1) and third (Q3) quartiles. Q1 indicates that twenty-five percent of data fall below the lower quartile. Q3 indicates that seventy-five percent of
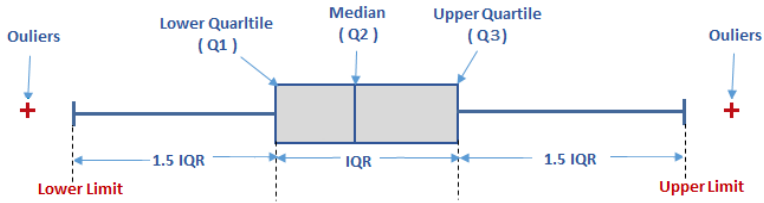
Figure 3.9: Boxplot example

the data fall below the upper quartile. The central mark (Q2) indicates the median of the data set. The two horizontal lines that extend from the front and back of the box are called whiskers. The whiskers tell us essentially the spread of all the data, the maximum and the minimum (not considering outliers) of the data set. The difference between the third and first quartile (Q3 - Q1) is called the interquartile range or IQ. Values higher than Q3+1.5*IQ or lower than Q1-1.5*IQ are considered outliers and are displayed with a red + sign.

Chapter 4

Results

This chapter shows and compares the measurements and calculations obtained during this research. First, field measurements are presented by boxplots. The results from the calculations done in order to be able to calculated the sound levels are also presented in this section. Finally, the results from the comparison between measurements and calculations are also presented by boxplots.

4.1 Field measurements

Two measurement series were carried in the same geographical area. In series 1, measurements were taken every two minutes over 2 days and 19 hours. In series 2, measurements were taken also every two minutes but over 3 days and 22 hours. Figures 4.1 and 4.2 show the variation and distribution of the fast, A-weighted (L_{AF}) measurements in both series.

Measurements were divided into two groups; measurements taken in favorable conditions and in homogeneous conditions as shown in Figures 4.3 and 4.4. Homogeneous conditions refers to wind speeds at the receiver between $-1\,\mathrm{m/s}$ and $1\,\mathrm{m/s}$. Favorable conditions refers to wind speeds between $1\,\mathrm{m/s}$ and $5\,\mathrm{m/s}$. The wind speed at the receivers were estimated, as described in section 3.4.1. Figures 4.3 and 4.4 show that the measured sound levels in favorable conditions were not always higher than measurements in homogeneous conditions, as theory suggests. Therefore, when comparing measurements with calculations in the following sections, the data will not be divided in neither homogeneous nor favorable conditions.
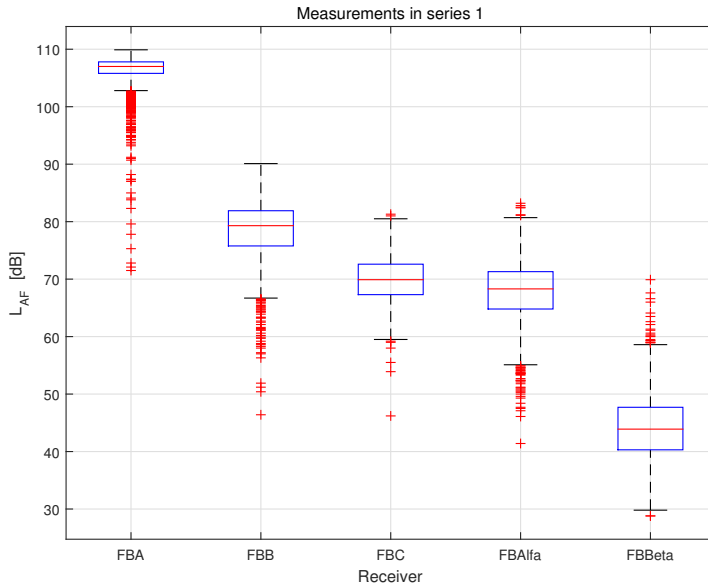
Figure 4.1: Field measurements in series 1
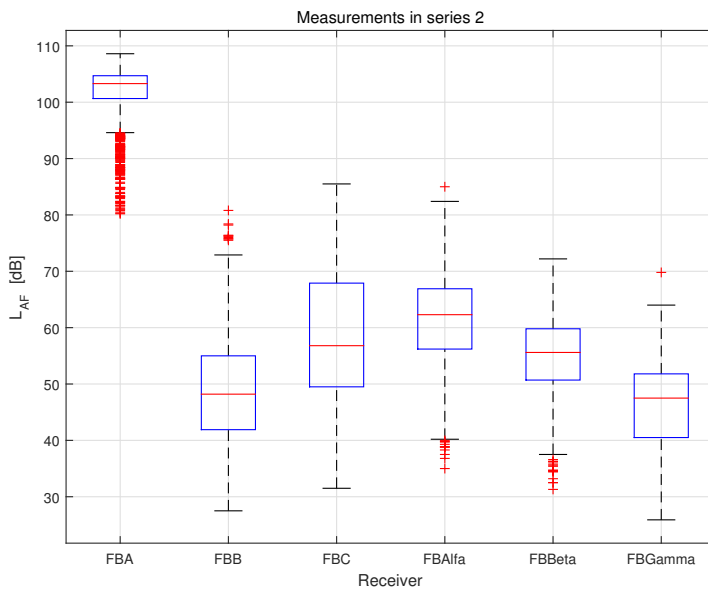
Figure 4.2: Field measurements in series 2
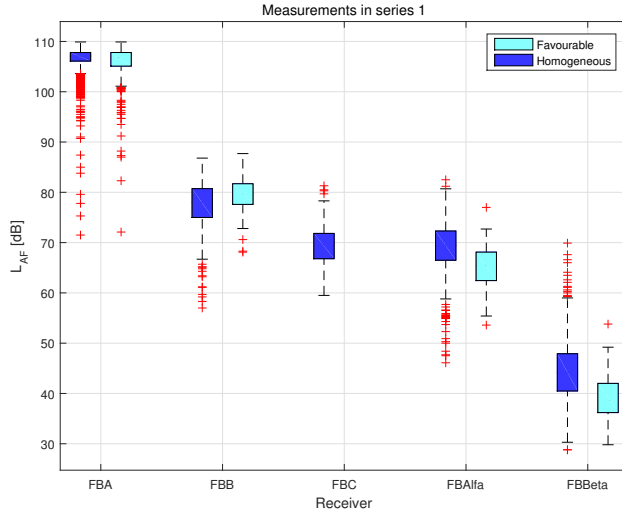
Figure 4.3: Measurements in series 1. Homogeneous: wind speed between $-1\,\mathrm{m/s}$ and $1\,\mathrm{m/s}$. Favorable: wind speed between $1\,\mathrm{m/s}$ and $5\,\mathrm{m/s}$. There is no boxplot for measurements in favorable conditions for receiver 3-FBC because the estimated wind speed were not in the range $\in [1, 5]$
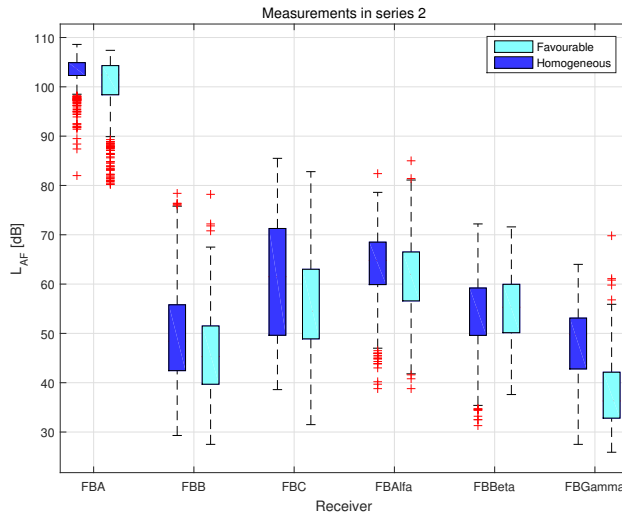

Figure 4.4: Measurements in series 2. Homogeneous: wind speed between $-1\,\mathrm{m/s}$ and $1\,\mathrm{m/s}$. Favorable: wind speed between $1\,\mathrm{m/s}$ and $5\,\mathrm{m/s}$
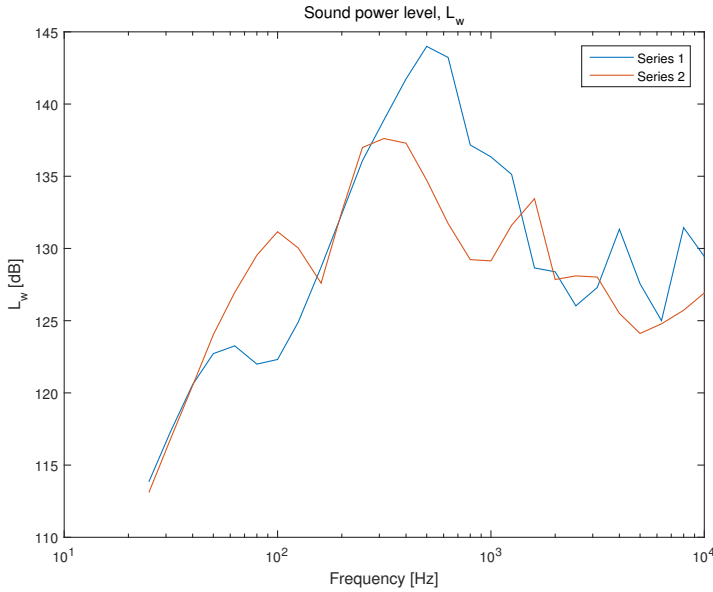
Figure 4.5: Calculated sound power level for series 1 and series 2

4.2   Calculations

In order to calculate the sound pressure level for the different propagation models, several calculations such as sound power level and directivity were computed. The following sections present some of these results.

Sound power level

Sound power level was calculated based on measurements in one-third octave bands from the receiver nearest to the source. Based on the two measurement series, two sound power levels were computed. Figure 4.5 shows the calculated power level for both series. Even though the same source was used in both measurement series, there are slightly differences in the power level at some frequencies. Figure 4.5 shows also that the gas cannon has highest energy at frequencies around 400 Hz–700 Hz which means that the sound power level will dominate the most at these frequencies.
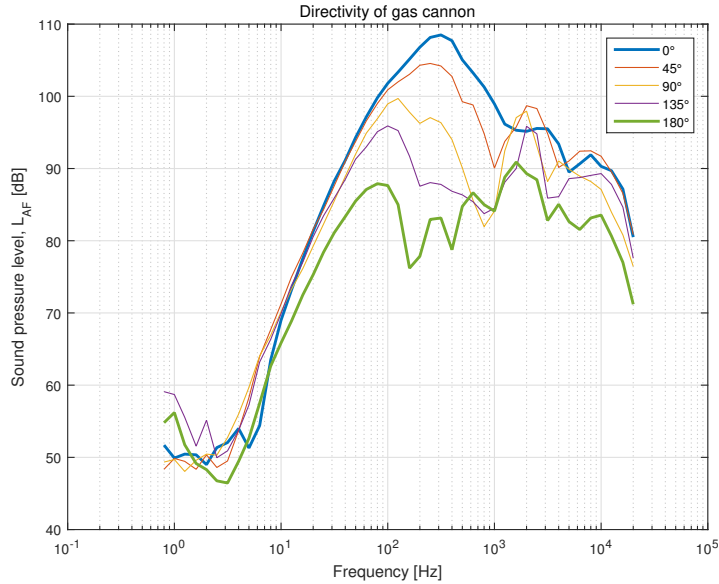
Figure 4.6: Directivity of gas cannon at different angles

Angle	0°	45°	90°	135°	180°
L_{AF} **[dB]**	111.25	108.70	104.75	102.45	98.90

Table 4.1: Fast, A-weighted measured values at different angles

Source directivity

Since not all the microphones were placed in front of the source, directivity of the source was taken into account when calculating sound levels at each receiver. Figure 4.6 shows the average of measurements in one-third octave band taken at each angle. The measurements at angles 0° and 180° are plotted with thicker lines to easily see the sound level difference between the two. Table 4.1 shows the average of fast, A-weighted measurements at each angle. From Table 4.1, it can be seen that there is approximately 12 dB sound level difference between 0° and 180°. The same difference should be shown in measurements and calculations where source and receiver are located at 180° difference and at the same distance from the source.
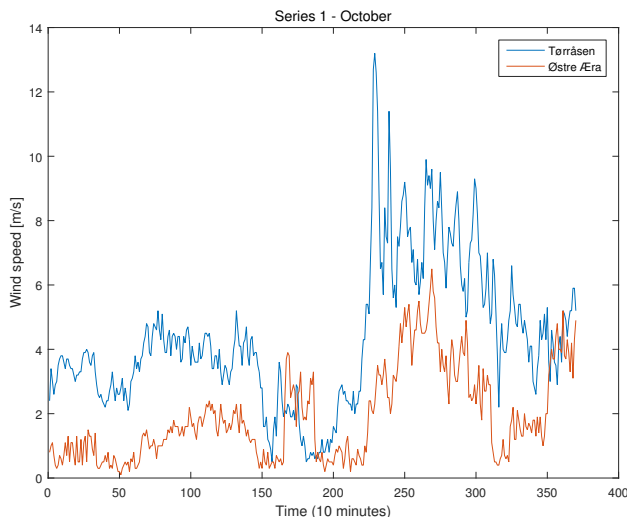
Figure 4.7: Wind speed measured in Tørråsen and Østre Æra in series 1

Correlation, ρ	Series 1	Series 2
ρ, wind speed	0.5634	0.3762
ρ, wind direction	0.2767	0.4211

Table 4.2: Correlation coefficient of wind direction between Tørråsen and Østre Æra weather station

Correlation wind speed

When calculating the sound levels with the Nord2000 implementation, wind speed is part of the input parameters. The wind speed at each receiver was estimated based on the measurements collected from the weather station nearest the measurement area, Tørråsen. In order to check how valid this approach is, the correlation of wind speed and wind direction between the two weather station nearest to the measurement area were computed. Figures 4.7 and 4.8 show the correlation of the wind speed between two weather stations in both measurement series.

Table 4.2 shows the correlation coefficients, ρ, based on Pearson correlation coefficient for wind speed and wind direction for both series. The values of the coefficients can range from -1 to 1, with -1 representing a direct, negative correlation, 0 representing no correlation, and 1 representing a direct, positive correlation.
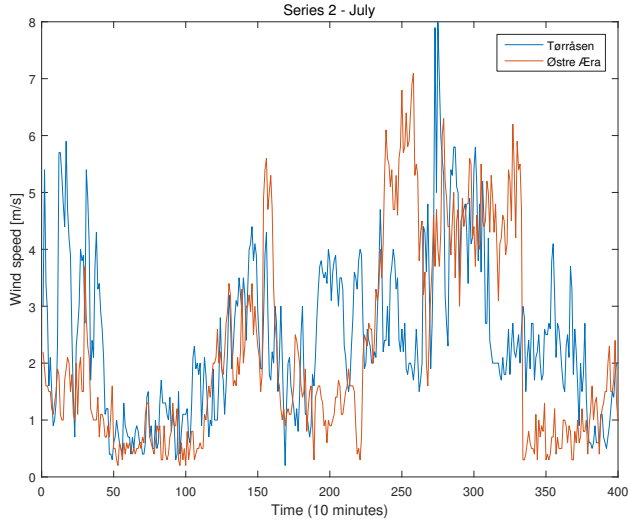
Figure 4.8: Wind speed measured in Tørråsen and Østre Æra in series 2

4.3 Comparison of calculations and measurements

To study the precision of the different propagation models, the error level, L_{error}, of the calculations is computed. The error level plotted in the following sections is based on the difference between A-weighted measured values and calculated A-weighted values ($L_{error} = L_{A,meas} - L_{A,calc}$). This section shows the results from both series. The results from each propagation path (source-receiver geometry) are presented on one page by three figures. The first figure illustrates the terrain profile approximated by a number of straight lines segments as defined in the Nord2000 model (see Figure 2.9). Different colors are used to indicate the ground surface characteristic of each segment, e.g. forest, marsh or open areas. The second and third figure show the error level when assuming favorable and homogeneous conditions, respectively, for different propagation models. Additionally, the angle, θ_{diff}, between the source and each receiver is shown on the titles for each case.

It is important to note that the calculated error levels in favorable conditions from ISO 9613-2, NMPB-2008 and Harmonoise are not comparable to the error level obtained from the Nord2000 model. This is because the first mentioned models assume constantly favorable conditions, while Nord2000 calculations include both favorable and homogeneous conditions since it computes sound levels based on the meteorological measurements from the weather

station, Tørråsen.

In addition, there are no results from the ISO 9612-3 model when assuming homogeneous conditions since the model only assumes favorable conditions.

Receiver 1 - FBA $(\theta_{diff} = 0°)$
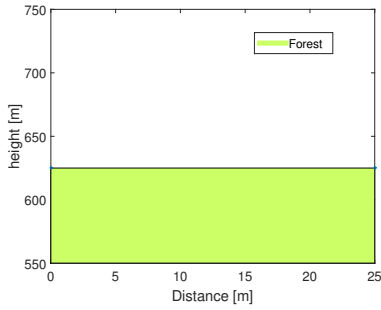
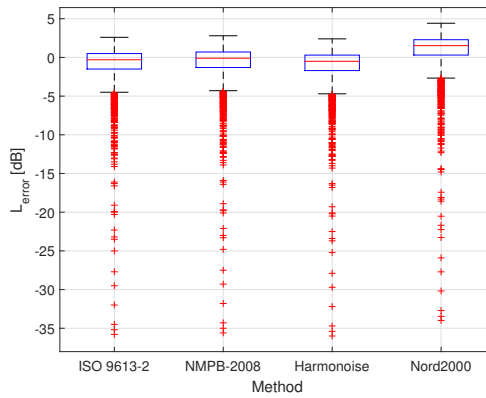Figure 4.9: Source-receiver geometry of receiver 1 - FBA in series 1

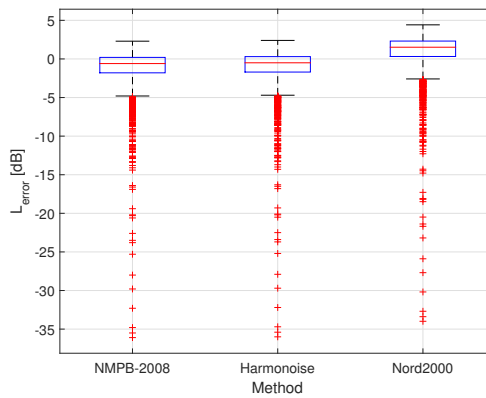Figure 4.10: Error level in favourable conditions for series 1

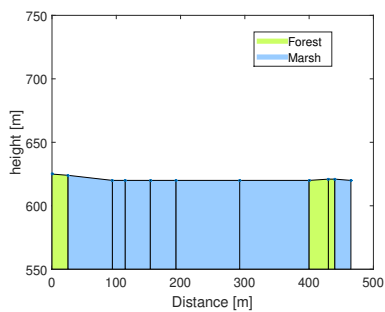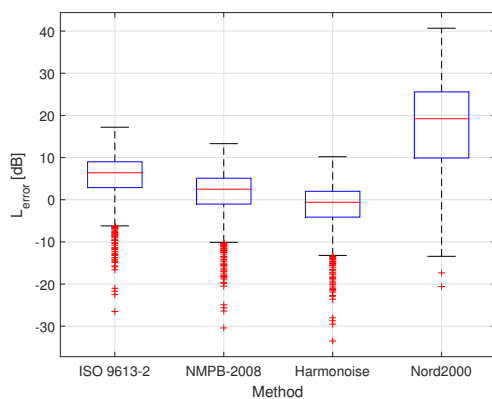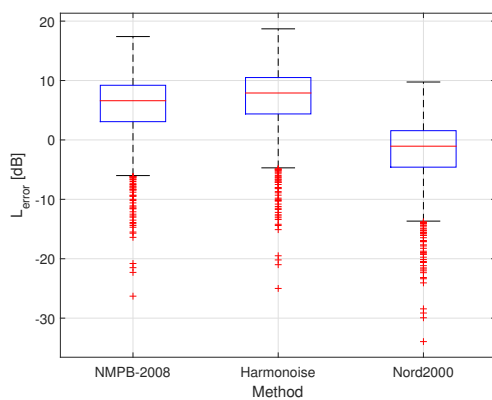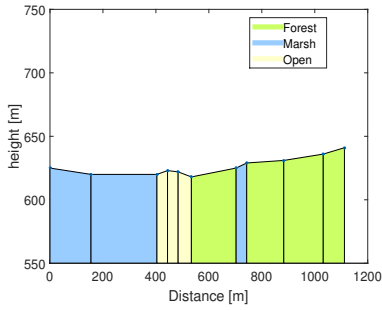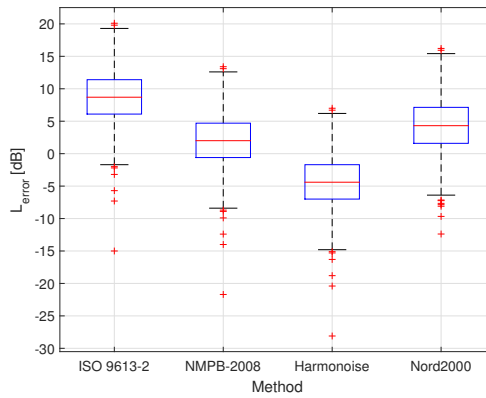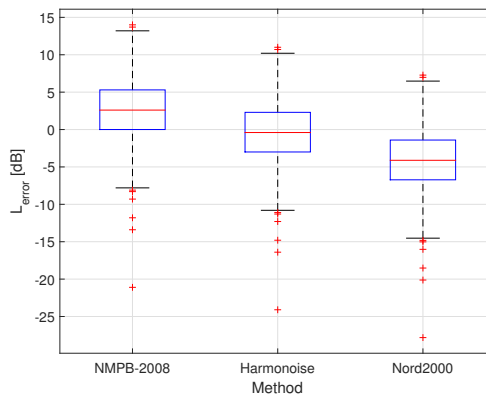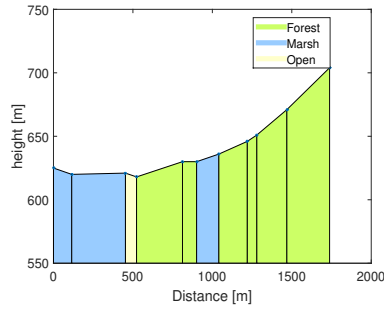Figure 4.11: Error level in homogeneous conditions for series 1

Receiver 2 - FBB $(\theta_{diff} = 28°)$

Figure 4.12: Source-receiver geometry of receiver 2 - FBB in series 1

Figure 4.13: Error level in favourable conditions for series 1

Figure 4.14: Error level in homogeneous conditions for series 1

Receiver 3 - FBC $(\theta_{diff} = 25°)$

Figure 4.15: Source-receiver geometry of receiver 3 - FBC in series 1

Figure 4.16: Error level in favourable conditions for series 1

Figure 4.17: Error level in homogeneous conditions for series 1

Receiver 4 - FBAlfa $(\theta_{diff} = 27°)$

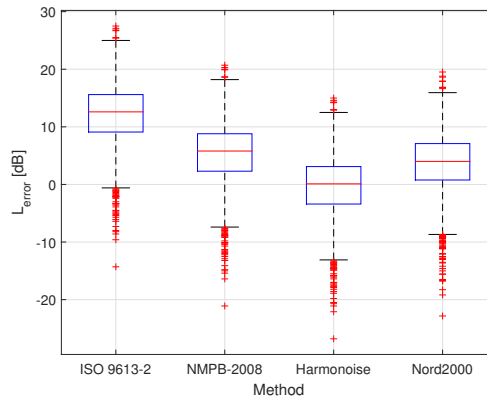Figure 4.18: Source-receiver geometry of receiver 4 - FBAlfa in series 1

Figure 4.19: Error level in favourable conditions for series 1
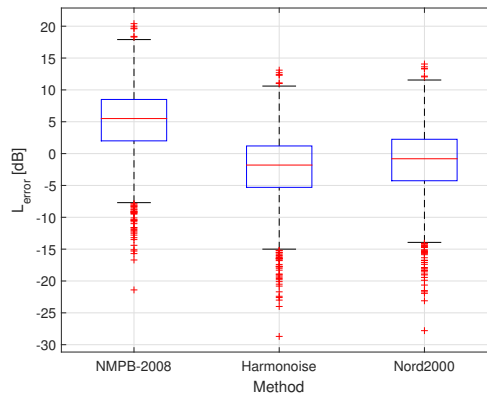

Figure 4.20: Error level in homogeneous conditions for series 1

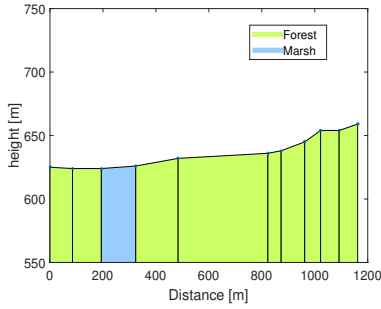**Receiver 5 - FBBeta** $(\theta_{diff} = 179°)$

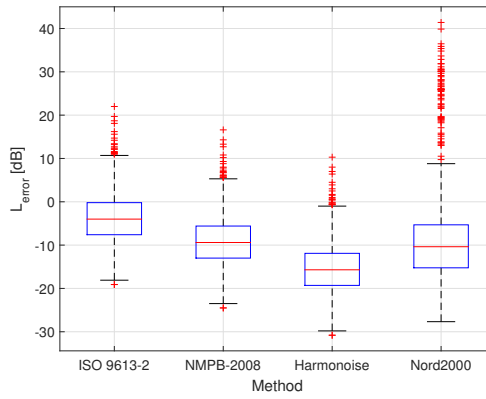Figure 4.21: Source-receiver geometry of receiver 5 - FBBeta in series 1

Figure 4.22: Error level in favourable conditions for series 1
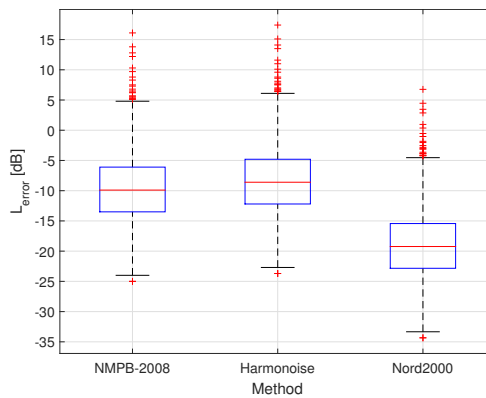

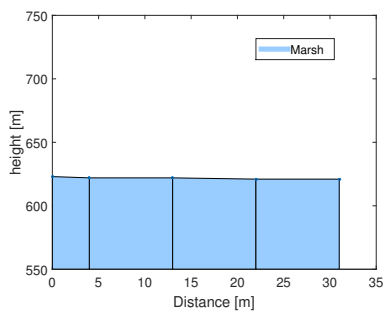Figure 4.23: Error level in homogeneous conditions for series 1

Receiver 1 - FBA $(\theta_{diff} = 0°)$

Figure 4.24: Source-receiver geometry of receiver 1 - FBA in series 2

Figure 4.25: Error level in favourable conditions for series 2

Figure 4.26: Error level in homogeneous conditions for series 2

Receiver 2 - FBB $(\theta_{diff} = 86°)$

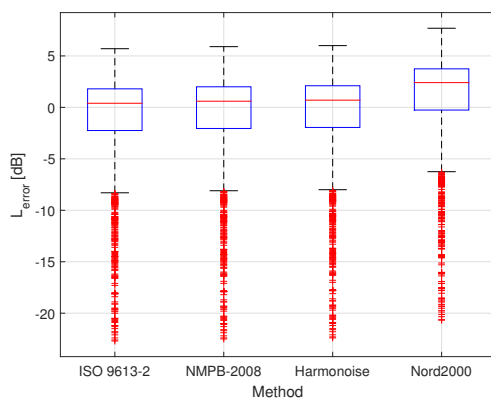Figure 4.27: Source-receiver geometry of receiver 2 - FBB in series 2

Figure 4.28: Error level in favourable conditions for series 2

Figure 4.29: Error level in homogeneous conditions for series 2

Receiver 3 - FBC ($\theta_{diff} = 39°$)

Figure 4.30: Source-receiver geometry of receiver 3 - FBC in series 2

Figure 4.31: Error level in favourable conditions for series 2

Figure 4.32: Error level in homogeneous conditions for series 2

Receiver 4 - FBAlfa $(\theta_{diff} = 7°)$
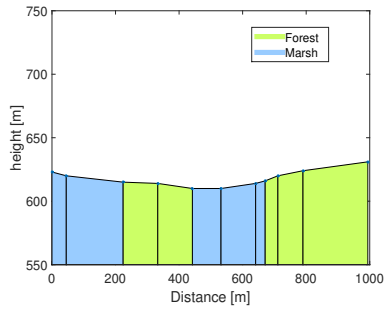
Figure 4.33: Source-receiver geometry of receiver 4 - FBAlfa in series 2
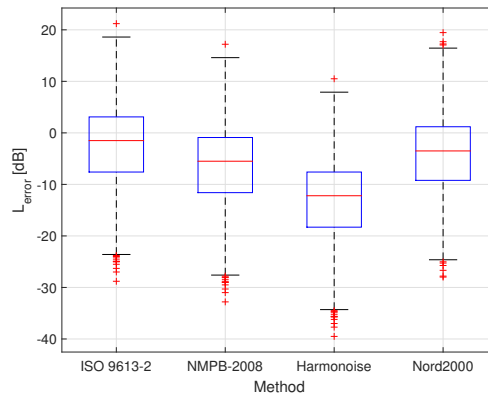
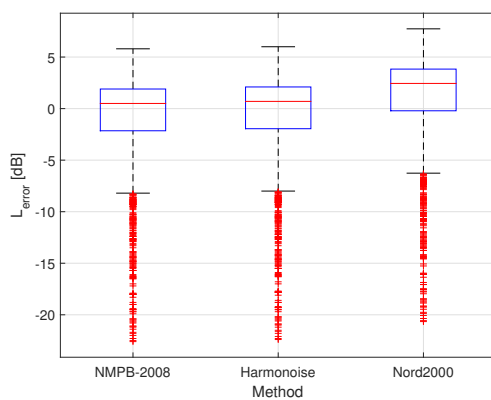Figure 4.34: Error level in favourable conditions for series 2
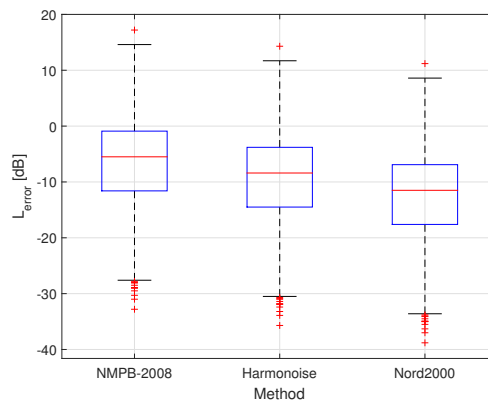
Figure 4.35: Error level in homogeneous conditions for series 2

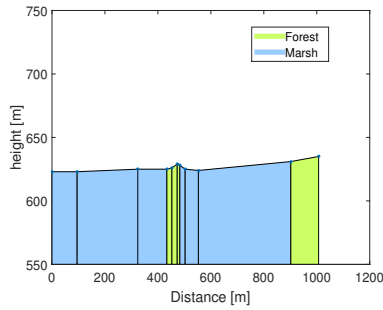**Receiver 5 - FBBeta** ($\theta_{diff} = 49°$)
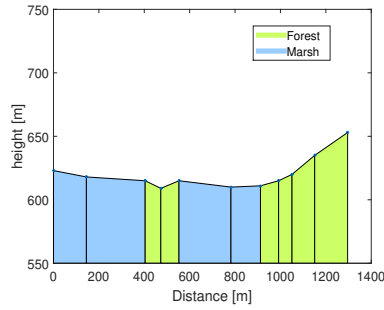
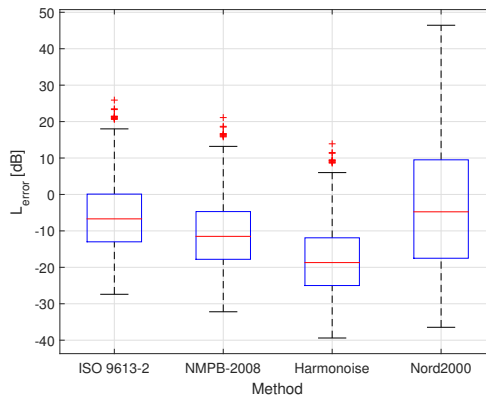Figure 4.36: Source-receiver geometry of receiver 5 - FBBeta in series 2
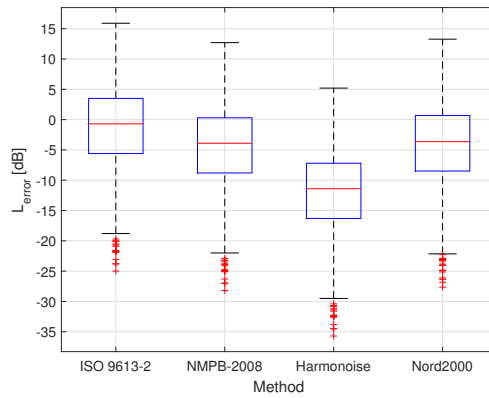
Figure 4.37: Error level in favourable conditions for series 2
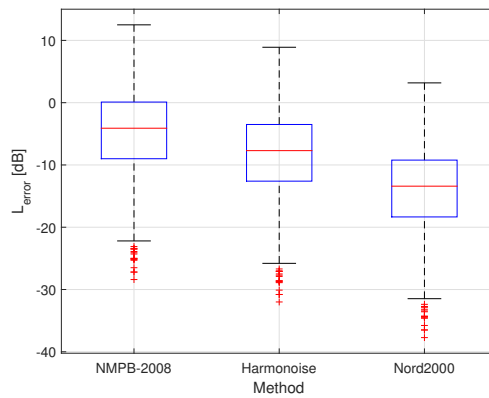
Figure 4.38: Error level in homogeneous conditions for series 2

Receiver 6 - FBGamma ($\theta_{diff} = 103°$)
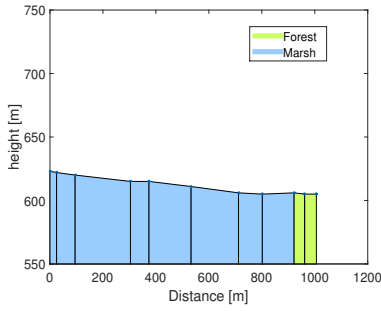
Figure 4.39: Source-receiver geometry of receiver 6 - FBGamma in series 2
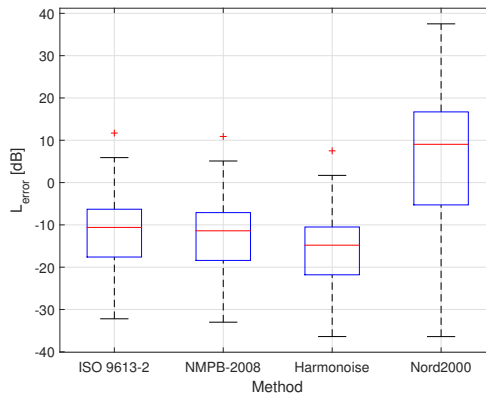
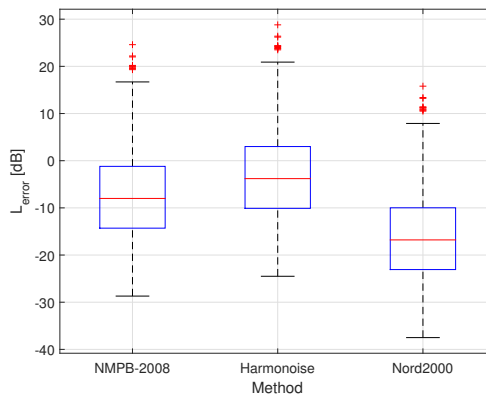Figure 4.40: Error level in favourable conditions for series 2

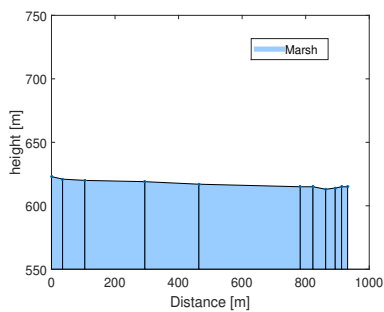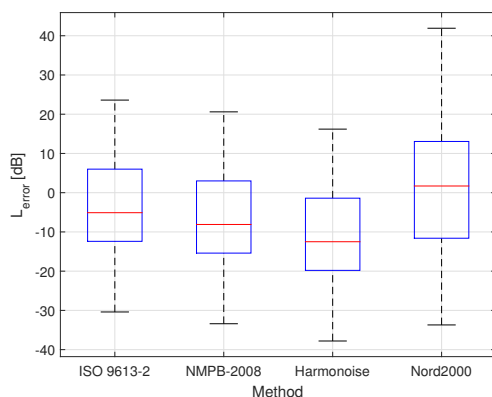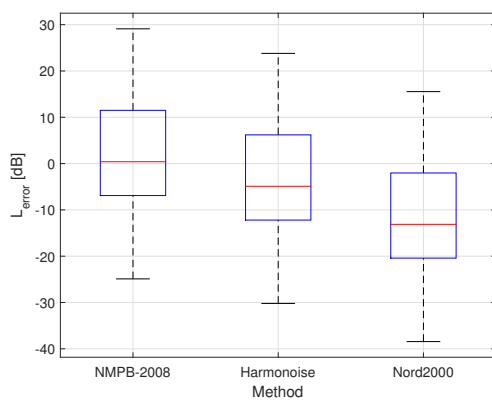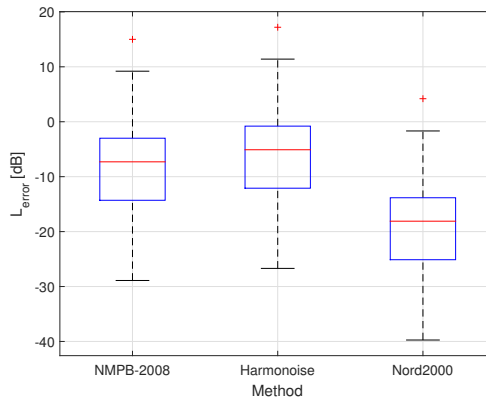Figure 4.41: Error level in homogeneous conditions for series 2

4.3.1   Average deviation

In addition to the graphical results presented in the previous section. The average deviation, L_{avg}, computed by Equation 3.3 from all the cases and for each model is presented in Table 4.3.

Tables 4.4 and 4.5 show the median value from all error levels computed for each source-receiver propagation cases in both series.

Method	Average deviation
ISO 9613-2	5.18
NMPB-2008	5.08
Harmonoise	6.43
Nord2000	7.57

Table 4.3: Average deviation between calculated A-weighted values from the four model predictions and measurements

Favorable	ISO 9613-2	NMPB-2008	Harmonoise	Nord2000
FBA	-0,30	-0,10	-0,50	1,52
FBB	6,40	2,50	-0,60	19,21
FBC	8,70	2,00	-4,40	4,31
FBAlfa	12,60	5,80	0,10	4,00
FBBeta	-4,00	-9,40	-15,70	-10,37
Homogeneous				
FBA	-	-0,60	-0,50	1,52
FBB	-	6,60	7,90	-1,05
FBC	-	2,60	-0,40	-4,11
FBAlfa	-	5,50	-1,80	-0,81
FBBeta	-	-9,90	-8,60	-19,24

Table 4.4: Error levels for each model and propagation path in series 1

Favorable	ISO 9613-2	NMPB-2008	Harmonoise	Nord2000
FBA	0,40	0,60	0,70	2,41
FBB	-6,70	-11,50	-18,70	-4,76
FBC	-5,10	-8,10	-12,50	1,71
FBAlfa	-1,50	-5,50	-12,20	-3,50
FBBeta	-0,70	-3,90	-11,40	-3,64
FBGamma	-10,60	-11,40	-14,80	9,05
Homogeneous				
FBA	-	0,50	0,70	2,44
FBB	-	-8,00	-3,80	-16,79
FBC	-	0,40	-4,90	-13,12
FBAlfa	-	-5,50	-8,40	-11,50
FBBeta	-	-4,10	-7,70	-13,41
FBGamma	-	-7,30	-5,10	-18,11

Table 4.5: Error levels for each method and propagation path in series 2

Chapter 5

Discussion

5.1 Measurements

Figures 4.1 and 4.2 show boxplots of field measurements in series 1 and series 2. Here, it can be seen that measurements in series 2 have larger variability (whiskers extends longer from the quartiles and the length of the boxes are larger) than in series 1. This may be due to more variations in the weather conditions during measurement in series 2 or other sound sources in the area. Figures 4.1 and 4.2 show several outliers in receiver FBA. Since FBA is the receiver nearest to the source, the measurements are expected to be precise and without so many variations. A possible reason for this may be possible defects in the functionality of the cannon. The cannon might not have fired correctly every single time producing lower sound levels.

From Figure 3.2 or Figures 4.15 and 4.21, it can be seen that receivers FBC and FBBeta were both located at approximately 1100 m from the source. Receiver FBBeta was located behind the source while receiver FBC was situated in front of the cannon. The angle difference between the two receivers was about 200°. Based on the source directivity measurements carried out by Forsvarsbygg, the difference between the sound level measured at 0° and 180° was about 12 dB (see Table 4.1). This does not agree with the field measurements which show a difference of 25 dB between receiver FBC and FBBeta as shown in Figure 4.1. In addition to the 20° difference between the field measurements and the directivity measurements, the meteorological conditions during measurements may be the reason for a difference of over 10 dB. When calculating the directivity correction for the cannon, it was assumed

that the calibration measurements are reliable results and were therefore used in further calculations.

After estimating the wind speed based on the wind conditions measured in Tørråsen at each receiver, the data was divided into two groups; measurements in homogeneous and favorable conditions. Figures 4.3 and 4.4 show measurements in favorable (wind speed between $1\,\text{m/s}$ and $5\,\text{m/s}$ and homogeneous conditions (wind speed between $-1\,\text{m/s}$ and $1\,\text{m/s}$ in series 1 and 2, respectively. It can be seen no clear connection between the measured sound levels and wind conditions. As mentioned in Section 2.1.2, theory in outdoor sound propagation refers to higher sound levels in downwind conditions (favorable) than in upwind or homogeneous conditions. This can not be seen in all the source-receiver cases, which suggest that the estimated wind speed values do not represent the wind speeds that were in the measurement area during the measurements. Additionally, as can be seen from Figure 4.3 the receiver FBC is the only receiver without measurements in favorable conditions. This is a suspect result since in series 1 all the receivers were located in almost a straight line in front of the source (see Figure 3.3). Thus, it does not make sense that only in receiver FBC the wind conditions were only homogeneous, at least considering relatively flat terrain in the area.

In addition, the correlation of the wind speed and wind direction between the two weather stations nearest to the measurement area were computed to check the stability of the wind conditions in the area. Table 4.2 shows the correlation coefficients for wind direction and wind speed in both series. The correlation of wind speed between both weather stations is around 0.6 in series 1, which means a moderate positive relationship. While in series 2, the correlation coefficient is 0.4 referring to a weaker relationship. When it comes to the correlation of the wind direction, the correlation coefficients show a weak positive relationship between the two weather stations. As expected, the wind conditions seem to vary in the area, and it would not be a good assumption either to assume the same wind conditions in the measurement area as in Tørråsen. The wind conditions used in the calculation by the models were, therefore, the estimated wind speed. The data was not divided into homogeneous and favorable conditions when comparing measurements and calculations.

5.2   Comparison of measurements and calculations

When trying to analyze and study the results from Figures 4.10–4.41, there seems not to be a clear pattern when comparing the error levels between

the models and each source-receiver geometry. It seems that the results vary randomly in many cases. However, there are some cases that stand out and will be discussed in this section.

Figure 4.10 shows the results in favorable conditions from receiver FBA in series 1. The receiver was located 25 m away from the source. As can be seen from Figure 4.9, the terrain was flat and ground surface in the area was forest. Figures 4.10 and 4.11 show that all models agree with each other and the error level from all the models is nearly 0 dB. In addition, several outliers can be seen in the calculations from all the models in both series. As mentioned before, this might be because the gas cannon did not fire properly all the time. The same applies to the results obtained from receiver 1-FBA in series 2, as shown in Figures 4.25 and 4.26. These results are as expected since the power level of the source was estimated based on the measurements from the receiver FBA in both series. Therefore, this result does not imply that all the models manage to calculate the sound levels at distance between 25 m and 30 m without any deviation.

Figures 4.13 and 4.14 show the results from receiver 2 - FBB in homogeneous and favorable conditions in series 1. As shown in Figure 4.12, the receiver is located 50 m away from the source and the terrain is relatively flat which mostly consist of marsh. From Figures 4.14 and 4.13 it can be seen that deviations between the models start to appear. The receiver is further away and more propagation factors affect the propagation of sound. In favorable conditions (Figure 4.13), sound levels predicted by Harmonoise model seems to agree very well with the measurements, giving an error level of nearly 0 dB. While NMPB-2008 gives an error level of approximately 4 dB, and ISO 9613-2 gives approximately 7 dB. However, calculations with Nord2000 show an error level of about 20 dB, where the model underestimates the sound level significantly. Nord2000 is an advanced propagation model, and such a high error level is therefore not expected. The reason for this strange result is not clear and no explanation can be found in the Nord2000 model description. A possible reason that could explain such deviation is that parameters used for describing weather conditions do not represent the actual weather conditions during the measurements. This is because, as shown in Figure 4.11, Nord2000 predicts the sound level much better when assuming homogeneous conditions, giving an error level of nearly 0 dB. This result is not so convincing either since both NMPB-2008 and Harmonoise gave an error level of approximately 6 dB, which are slightly higher than both methods gave in favorable conditions, indicating that the weather conditions during the measurements were generally favorable conditions.

Further, it can be observed a pattern among the results from ISO 9613-2, NMPB-2008 and Harmonoise when assuming favorable conditions in the calculations of both series. In most of the cases, ISO 9613-2 gives the highest

value, then NMPB-2008 and at last Harmonoise. This may imply that ISO 9613-2 underestimate the sound levels the most among these models.

Figures 4.22 and 4.23 show the results from receiver FBBeta in favorable and homogeneous conditions, respectively. FBBeta was located behind the cannon at approximately 1100 m from the source and the terrain was not completely flat, but had a slightly positive slope, as shown in Figure 4.21. In this case, all the models overestimated the sound level. A possible explanation for such result is that the estimated directivity corrections are not representative in this case. The directivity of the source could have been affected by meteorological conditions during the field or calibration measurements. The same results are obtained in series 2, where most of the receivers were not located in front of the cannon. In series 2, the calculations were in most of the cases significantly overestimated giving error levels up to 20 dB. In addition, the two receivers located with the largest angle difference were receivers FBB and FBGamma (see Figure 3.3). The results from these two receivers gave the absolutely highest error levels.

Overall, the results varied without a clear trend, making it difficult to draw conclusions about what method and at which situations they predict the sound level best. Based on the average of all the results presented in Table 3.3, the results show that NMPB-2008 gives an average error level of 5.08 dB, ISO 9613-2 with 5.18 dB, Harmonoise 6.43 dB and Nord2000 7.57 dB. This indicates that, in the absence of on-site meteorological information, NMPB-2008 on average predicts the sound levels better which agrees with the result presented in an earlier study from 2014 [15].

Chapter 6

Conclusion

The overall purpose of this work was to determine the reliability and precision of four different models when studying impulse noises in the atmosphere. Results calculated by ISO 9613-2, NMPB-2008, Harmonoise and Nord 2000, have been compared with field measurements.

The propagation distances in the field measurements varied between 20 m and 2 km. Since the meteorological conditions were not measured in the immediate vicinity of the measurements, the wind speed at each receiver was estimated based on measurements collected from the weather station nearest to the measurement area. These estimations did not seem to be representative for the meteorological conditions at each receiver. The error level, i.e. the difference between measurements and calculations, was computed in order to determine the accuracy of the models.

The results did not show a clear pattern when studying the error level for each model and propagation path. However, the average of all the error levels obtained for each model, showed that in the absence of on-site meteorological information, NMPB-2008 on average predicts the sound levels better than the other models. The model with the largest average deviation was Nord2000 with an average error level of approximately 7.6 dB. A possible explanation for such result, is that the parameters used for describing weather conditions in the Nord2000 implementation are not representative for the weather conditions during the measurements.

Further analysis and measurements are needed to be able to determine which model can with good accuracy predict sound level from impulse noises in the atmosphere. There are several improvements that can be done in order to get more reliable results. Measurements of the weather conditions should be

closer to the measurement area. Measurements over a longer period of time will give more accurate data. A more detailed estimation of temperature gradients can also be done by taking into account the distance between the weather stations and the measurement area.

Bibliography

[1] Saeed V Vaseghi. *Advanced digital signal processing and noise reduction*, chapter 12. John Wiley & Sons, second edition, 2000.

[2] Klima og miljødepartementet. Retningslinje for behandling av støy i arealplanlegging. 2012.

[3] Erik Salomons. *Computational Atmospheric Acoustics*. Springer Science & Business Media, 2012.

[4] Paul Filippi, Aime Bergassoli, Dominique Habault, and Jean Pierre Lefebvre. *Acoustics: basic physics, theory, and methods*. Academic Press, 1998.

[5] NT ACOU 099. Shooting ranges: Prediction of noise. *2nd ed. Helsinki*, 2002.

[6] JM Wunderli, R Pieren, and K Heutschi. The Swiss shooting sound calculation model sonARMS. *Noise Control Engineering Journal*, 60(3): 224–235, 2012.

[7] ISO 9613-2. Acoustics - Attenuation of sound during propagation outdoors - Part 2: General method of calculation. Technical report, International Standardization Organization, 1996.

[8] Erik Salomons, Dirk Van Maercke, Jérôme Defrance, and Foort de Roo. The Harmonoise sound propagation model. *Acta acustica united with acustica*, 97(1):62–74, 2011.

[9] Jérôme Defrance, Erik Salomons, Ingrid Noordhoek, Dietrich Heimann, Birger Plovsing, Greg Watts, Hans Jonasson, Xuetao Zhang, Eric Premat, Isabelle Schmich, et al. Outdoor sound propagation reference model developed in the European Harmonoise project. *Acta Acustica united with Acustica*, 93(2):213–227, 2007.

[10] Birger Plovsing. Nord2000. Comprehensive outdoor sound propagation model. part 1: Propagation in an atmosphere without significant refraction. Technical report, Delta Acoustics & Electronics, 2006.

[11] Birger Plovsing. Nord2000. Comprehensive outdoor sound propagation model. part 2: Propagation in an atmosphere with refraction. Technical report, Delta Acoustics & Electronics, 2006.

[12] Birger Plovsing. Proposal for nordtest method: Nord2000 - Prediction of outdoor sound propagation. Technical report, Delta Acoustics & Electronics, 2007.

[13] Guillaume Dutilleux, Jérôme Defrance, David Ecotière, Benoit Gauvreau, Michel Bérengier, Francis Besnard, and Emmanuel Le Duc. NMPB-routes-2008: the revision of the French method for road traffic noise prediction. *Acta Acustica united with Acustica*, 96(3):452–462, 2010.

[14] Franois Abbaléa, Savine Andry, Marine Baulac, Michel Bérengier, Bernard Bonhomme, Jérme Defrance, Jean Pierre Deparis, Guillaume Dutilleux, David Ecotiére, Benoît Gauvreau, Vincent Guizard, Fabrice Junker, Hubert Lefévre, Vincent Steimer, Dirk Van Maercke, and Vadim Zoubof. Road noise prediction – 2: Noise propagation computation method including meteorological effects (NMPB 2008). Technical report, 2009.

[15] Cédric Foy, David Ecotiere, and Guillaume Dutilleux. Comparison of 3 engineering methods for outdoor sound propagation. *DAGA Oldenburg*, 2014.

[16] Gunnar Birnir Jónsson. A comparison of two numerical models for outdoor sound propagation. Master's thesis, Technical University of Denmark, DTU, DK-2800 Kgs. Lyngby, Denmark, 2007.

[17] Johan Gisaeus. Calculation of outdoor sound propagation by engineering methods.

[18] Keith Attenborough, Kai Ming Li, and Kirill Horoshenkov. *Predicting outdoor sound*. CRC Press, 2006.

[19] Louis C Sutherland and Gilles A Daigle. *Atmospheric Sound Propagation*, volume 28. Wiley: New York, NY, USA, 1998.

[20] Jens Jørgen Dammerud. Elektroakustikk. *4. utgave*, 2013.

[21] André Felipe Oliveira. The effect of wind and turbulence on sound propagation in the atmosphere. Master's thesis, Technical University of Lisbon, 2012.

[22] Keith Gibbs. Schoolphysics - Diffraction, 2009. URL `http://www.schoolphysics.co.uk/index.php`.

[23] Erlend Magnus Viggen, Herold Olsen, and Truls Gjestland. Small arms noise mapping method in Norway and comparable nations. Project No. 102007702, March 2016.

[24] Jørgen Kragh, Hans Jonasson, Birger Plovsing, Ari Sarinen, SÅ Storeheier, and G Taraldsen. User's guide Nord2000 road. *Delta, SINTEF, SP and VTT*, 2006.

[25] ME Delany and EN Bazley. Acoustical properties of fibrous absorbent materials. *Applied acoustics*, 3(2):105–116, 1970.

[26] John Klinkby. Nord2000 VS the existing Nordic propagation models. 2002.

[27] Jørgen Kragh. Traffic noise prediction with Nord2000 - an update. In *Proceedings of Acoustics*, 2011.

[28] Scaring birds. Product: DBS E auto cannon, 2012. URL `http://www.scaringbird.com`.

[29] Universal Transverse Mercator coordinate system. Universal transverse mercator coordinate system (UTM) — Wikipedia, the free encyclopedia, 2017. URL `https://en.wikipedia.org/wiki/Universal\_Transverse\_Mercator\_coordinate\_system`. [Online; accessed 20-April-2017].

[30] Kartverket. Norgeskart, lla 9888. URL `https://www.norgeskart.no/\#5/272763/7041181`.

[31] Dirk Van Maercke. CNOSSOS-EU User's and programmer's guide. Task 2: Propagation software modules. 2014.

[32] Jørgen Kragh. User's guide Nord2000 road. Technical report, Delta Acoustics & Electronics, 2006.

[33] MathWorks. Box plots. URL `https://ch.mathworks.com/help/stats/box\-plots.html`.